Molecular Orbitals Support Energy-Stabilizing 'Bonding' Nature of Bader's Bond Paths

Ignacy Cukrowski,* Jurgens H. de Lange, Daniël M. E. van Niekerk and Thomas G. Bates

Department of Chemistry, Faculty of Natural and Agricultural Sciences, University of Pretoria, Lynnwood Road, Hatfield, Pretoria 0002, South Africa

Supporting Information

*Correspondence to: Ignacy Cukrowski

E-mail: ignacy.cukrowski@up.ac.za

Content

Page

Part 1. Theoretical background

The MO-ED method S3

The MO-DI method S8

Part 2. Cartesian coordinates of molecules studied

Planar biphenyl S12

Twisted biphenyl S13

Li_4H_4 S14

Part 3. Canonical molecular orbitals in biphenyl

Planar biphenyl S15

Twisted biphenyl S22

Part 4. Data pertaining to covalent bonds in biphenyl

MO-ED and MO-DI data S29

Decomposition of the total-ED at CP(C1,C12) and CP(C19,H22) S34

Part 5. Data pertaining to CP/MDP(H7,H18) in the planar/twisted biphenyl

MO-ED and MO-DI data S36

Decomposition of the total-ED at relevant CP/MDP(H7,H18) S41

Part 6. Data pertaining to H ··H density bridges in Li_4H_4

MO-ED and MO-DI data S43

Decomposition of the total-ED at the CP(H2,H5) S46

Part 1

A theoretical background

The MO-ED Method

The MO-ED method seeks to describe the total electron density, as well as its topology, in terms of molecular orbital density contributions. Specifically, we aim here to describe the presence of a density bridge, with its associated critical point, in terms of MO densities. To do so we will first review some preceding topics related to the topology of the electron density.

The topology of the electron density

Within the field of Quantum Chemical Topology (QCT), a critical point (CP) in the electron density (ED) at a coordinate $\mathbf{r}_c$ is a local maximum, minimum or a saddle point where the first derivative (and each of its three components) vanishes:

$$\nabla\rho(\mathbf{r}_c) = \mathbf{i}\frac{\partial\rho}{\partial x} + \mathbf{j}\frac{\partial\rho}{\partial y} + \mathbf{k}\frac{\partial\rho}{\partial z} = 0 \qquad (1)$$

Each CP is a local maximum or minimum along each of the three principle axes corresponding to maximum curvature. The type of CP can be determined by evaluating components of the Hessian matrix, which describe the partial second derivatives of the ED at $\mathbf{r}_c$:

$$\mathbf{A}(\mathbf{r}_c) = \begin{pmatrix} \frac{\partial^2\rho}{\partial x^2} & \frac{\partial^2\rho}{\partial x\partial y} & \frac{\partial^2\rho}{\partial x\partial z} \\ \frac{\partial^2\rho}{\partial y\partial x} & \frac{\partial^2\rho}{\partial y^2} & \frac{\partial^2\rho}{\partial y\partial z} \\ \frac{\partial^2\rho}{\partial z\partial x} & \frac{\partial^2\rho}{\partial z\partial y} & \frac{\partial^2\rho}{\partial z^2} \end{pmatrix} \qquad (2)$$

The Hessian matrix can be diagonalized to give three curvatures along the principle axes at $\mathbf{r}_c$, yielding three eigenvalues, λ_1, λ_2 and λ_3, and associated eigenvectors. The sign of each eigenvalue reveals whether $\mathbf{r}_c$ is a local minimum or maximum along the associated eigenvector, where positive and negative eigenvalues relate to local minima and maxima, respectively.

Each CP can be classified according to its partial first and second derivatives, and is given a rank, ω, and signature, σ. The rank determines the number of non-zero curvatures (eigenvalues of the Hessian matrix). In other words, a rank of (+3) indicates that a CP is a local maximum or minimum in all three principle axes. The signature is the algebraic sum of the signs of the

eigenvalues, and a signature of (–1) indicates that $\mathbf{r}_c$ is a local minimum in one axis but a local maximum in the remaining two axes (+1 –1 –1 = –1). While many CPs of rank 1 and 2 exist in any ED distribution, only a number of CPs of rank 3 will exist, subject to the Poincaré-Hopf relationship,[1] and rank 3 CPs are therefore of particular use in QCT.

The topology of the ED is generally dominated by the electrostatic attractive force between nuclei and electrons, and as such, every nuclear coordinate is marked by a (+3,–3) CP – a local maximum in all three principle axes. (+3,–1) CPs are often found between pairs of nuclei and are known as bond critical points (BCPs). CPs found within a ring of nuclei are (+3,+1) CPs, known as ring critical points (RCPs), and a CP enclosed by a number of ring critical points is always a (+3,+3) CP, known as a cage critical point (CCP).

QCT has revealed a peculiar property regarding the ED distribution between nuclei. A BCP is always observed at the interface between two zero-flux surfaces outside of the limit at infinity, *i.e.* interatomic zero-flux surfaces. Two gradient vectors originate at each of the enclosed nuclei and terminate at the BCP. The path defined by these two vectors is known as a density bridge (DB, also known as a *bond path* or a line path[2]). The ED is at a local maximum perpendicular to the DB at each and every coordinate of the DB. A DB is a remarkable yet still misunderstood property of the ED. The collection of DBs gives rise to a *molecular graph*, which defines QTAIM-based atomic connectivity.

Two of the eigenvalues of the Hessian matrix (λ_1 and λ_2) will be negative at each and every coordinate of a DB, indicating a negative partial second derivative along the principle vectors perpendicular to the DB itself. A negative partial second derivative at **r**, $\frac{\partial^2 \rho(\mathbf{r})}{\partial \mathbf{r}^2}$, can be seen as a measure of local *concentration* of the ED, in that the ED at **r** is greater than the average of its neighbouring coordinates along a specific vector.[7] Along the DB, the third eigenvalue of the Hessian matrix (λ_3) will always be positive, indicating a local *depletion* of ED. Generally, at a given coordinate **r** along an internuclear vector and as long the two nuclei are not part of a cage, $\lambda_1 < 0$ and $\lambda_3 > 0$. The sign of the remaining eigenvalue, λ_2, then generally determines whether ED is concentrated at **r** relative to its neighbouring environment, thereby forming an DB if a CP is present, or whether the ED is depleted. Such concentrations and depletions have been used extensively by both QTAIM and other QCT techniques, such as the Noncovalent Interactions (NCI) technique,[3,4] to indicate '*attractive*' or '*repulsive*' interactions. However, some of us

previously showed[5] that measures of ED concentration utilising λ_2 is only relative to the local environment where it is measured.

Cross-sections along λ_2–eigenvector

As stated above, the presence of a DB can be fully determined in most circumstances from investigation of i) the partial directional first derivative and ii) the sign of the partial directional second derivative of the ED along the eigenvector associated with the λ_2 eigenvalue of the Hessian matrix. We will henceforth refer to this eigenvector simply as the λ_2–eigenvector. We have previously noted[5,6] that the ED distribution, as well as decompositions of the ED, of cross-sections along this vector can provide tremendous information regarding *why* a DB for a particular chemical interaction is present or not. Specifically, the overall concentration or depletion of ED along the λ_2–eigenvector provides valuable information regarding the character of the interaction, and the individual concentration or depletion of ED decomposition products can provide insight into the underlying mechanics. Cross-sections along one of the other principle axes, *i.e.* λ_1– or λ_3–eigenvectors, can provide useful information regarding the ED concentration/depletion relative to different interatomic interactions.

Decomposition of ED and its topology in terms of MO densities

The ED can easily be decomposed in terms of canonical or natural molecular orbitals (MOs),

$$\rho(\mathbf{r}) = \sum_{i}^{N_{MO}} \nu_i |\chi_i(\mathbf{r})|^2 \qquad (3)$$

where χ_i is an MO with occupation ν_i. The coordinate $\mathbf{r}$ can be varied (specifically, in this case, along the λ_2–eigenvector) in order to measure the orbital contributions to the ED in a region of real-space, as well as then calculate partial directional first and second derivatives.

It is useful to define a consistent and universal coordinate, **r***, which can be used to quantify an orbital's ED contribution to any internuclear region in a transferable fashion. While there are potentially multiple different approaches to define such an **r***, we have decided to use the topology of the ED as a general guide. If a (3,–1) CP is present, then we define $\mathbf{r}^* = \mathbf{r}_c$, the coordinate of the CP. If a (3,–1) CP is not present, then we set **r*** to be the position of the minimum density point (MDP)[15], which is defined as the coordinate on an internuclear vector

where the ED is at a minimum. The MDP is well-defined for any given atom-pair, and the MDP and BCP often coincides to the same coordinate unless the corresponding DB is particularly bent.

Next, we consider the partial directional second derivatives along the λ_2–eigenvector of each MO density as measured at **r***, $\frac{\partial^2 \nu_i |\chi_i(\mathbf{r}^*)|^2}{\partial \lambda^2}$. We can label each MO as concentrating ED (negative second derivative), depleting ED (positive second derivative), non-contributing to the ED (in the case of an MO node) or removing ED (in the case of negative occupations in multi-reference wavefunctions). The ED at **r*** can then be defined in terms of MO components with different characters:

$$\rho(\mathbf{r}^*) = \rho_{\text{concentrating}}(\mathbf{r}^*) + \rho_{\text{depleting}}(\mathbf{r}^*) + \rho_{\text{non-contributing}}(\mathbf{r}^*) + \rho_{\text{removing}}(\mathbf{r}^*) \quad (4)$$

Each individual MO's character is therefore defined relative to a specific internuclear region, as opposed to a "net" character given based on inspection of molecular-wide isosurface or interference patterns of atomic orbitals.

The CP(r) function as a criteria for the presence of a DB

Using the above information regarding the decomposition of the ED distribution (Eq. 4), a similar decomposition can be performed for the partial directional first and second derivatives along the λ_2–eigenvector, as shown for the first derivative:

$$\partial\rho(\mathbf{r}^*) = \partial\rho_{\text{concentrating}}(\mathbf{r}^*) + \partial\rho_{\text{depleting}}(\mathbf{r}^*) + \partial\rho_{\text{non-contributing}}(\mathbf{r}^*) + \partial\rho_{\text{removing}}(\mathbf{r}^*) \quad (5)$$

For a DB to be present, Eq. 5 should be zero at some coordinate (specifically at a CP(3,–1)) somewhere on the λ_2–eigenvector. Naturally, this means that $\partial\rho(\mathbf{r})$ will approach zero in the vicinity of a CP or MDP; the net sign of $\partial\rho(\mathbf{r})$ is, however, numerically dependent and irrelevant for the following discussion. That means that individual terms in Eq. 5 will sum up to zero, or their sum will approach zero in the vicinity of a CP or MDP. $\partial\rho_{\text{non-contributing}}(\mathbf{r}^*)$ will always be zero (or numerically so), and, in the interest of simplicity, we can ignore $\partial\rho_{\text{removing}}(\mathbf{r}^*)$ as we are not dealing with any multi-determinant wavefunctions in this work. That leaves the interplay between the slopes of MOs that concentrate or deplete ED ($\partial\rho_{\text{concentrating}}(\mathbf{r}^*) +$

$\partial\rho_{\text{depleting}}(\mathbf{r}^*)$) that will determine whether $\partial\rho(\mathbf{r})$ crosses zero. The two possibilities which will lead to the formation of a DB is if i) both the slopes of concentrating and depleting contributions at **r*** are zero, or ii) the slopes of concentrating and depleting contributions at **r*** are equal, but opposite in sign. We already know that the signs of the partial second derivatives along the λ_2–eigenvector for the concentrating and depleting contributions are negative and positive, respectively, and for a DB to be present, the partial second derivative of the total ED is also negative ($\lambda_2 < 0$). Therefore, in the *vicinity* of a (3,–1) CP, the absolute gradient of the concentrating contributions will be greater than the absolute gradient of the depleting contributions, leading to the following conditions:

$\left|\partial\rho_{\text{concentrating}}(\mathbf{r}^*)\right| > \left|\partial\rho_{\text{depleting}}(\mathbf{r}^*)\right|$, in the vicinity of a (3,–1) CP

$\left|\partial\rho_{\text{concentrating}}(\mathbf{r}^*)\right| < \left|\partial\rho_{\text{depleting}}(\mathbf{r}^*)\right|$, outside the vicinity of a (3,–1), and

$\left|\partial\rho_{\text{concentrating}}(\mathbf{r}^*)\right| - \left|\partial\rho_{\text{depleting}}(\mathbf{r}^*)\right| = 0$, at a (3,–1) CP

The second condition will hold for most interactions of interest, regardless of whether a DB is present or not. If a DB is not present, then the first and third condition will not be met. If a (3,+1) CP is present, then the first condition will not be met. In order to evaluate the interplay of these effects, we have proposed a function for detecting DBs when measured along the λ_2–eigenvector:

$$CP(\mathbf{r}) = -sign(\partial\rho_{\text{depleting}}(\mathbf{r})) \cdot \left[\partial\rho_{\text{concentrating}}(\mathbf{r}) + \partial\rho_{\text{depleting}}(\mathbf{r}) + \partial\rho_{\text{removing}}(\mathbf{r})\right] \quad (6)$$

The *CP*(**r**) function simply returns the slope of the total ED (Eq. 5), but modified by the sign of the net slope of the nonbonding contributions. The *CP*(**r**) function will therefore also be equal to 0 at $\mathbf{r}^*$, if a DB is present. However, in the *vicinity* of a DB, a region along the λ_2–eigenvector will always exist where *CP*(**r**) is positive, in one or both directions, whereas *CP*(**r**) will always be negative if a BCP is absent.

The physical interpretation of the *CP*(**r**) function is simple: a DB will exist only if the combined slope of all MOs that concentrate ED in an inter-nuclear region is greater and opposite in sign than the combined slope of all MOs that deplete ED.

The MO-DI Method

The MO-DI method describes the QTAIM-defined delocalization index in terms of MO contributions to the pair-density. We will first review the basic concepts of how delocalization indices are calculated within QTAIM.

The integration of the overlap between all MO pairs over a QTAIM-defined atomic domain, Ω(A), can be written as a matrix associated with atom A, $\mathbf{S}^{\mathrm{A}}$, and is known as an *atomic overlap matrix* (AOM).[1] The elements of an N_{MO} by N_{MO} atomic overlap matrix,

$$S_{ij}^{\mathrm{A}} = \sum_{ij} \int_{\mathrm{A}} \sqrt{\nu_i}\sqrt{\nu_j}\chi_i^*(\mathbf{r})\chi_j(\mathbf{r})d\mathbf{r} \tag{7}$$

provide information on how each MO (diagonal elements) or a MO-pair (off-diagonal elements) contribute to the ED distribution of atom A. The atomic population (the average number of electrons found in the atomic basin) is therefore simply the sum of diagonal elements of the AOM:

$$N(\mathrm{A}) = tr(\mathbf{S}^{\mathrm{A}}) \tag{8}$$

The off-diagonal elements of each AOM, however, provide valuable information regarding the 2nd-order density distribution across the atom, *i.e.* how MOs interfere (de)constructively within Ω(A).[8,9] Such information can be used to indicate the degree of localization or delocalization of electrons within the atomic basin. Specifically, by integrating the pair density across two domains simultaneously, the total electron delocalization between electrons in each basin can be calculated:

$$\begin{aligned} \delta(\mathrm{A},\mathrm{B}) &= 2\left|-\sum_{ij}\int_{\mathrm{A}} d\mathbf{r}_1 \int_{\mathrm{B}} d\mathbf{r}_2\, \nu_i\nu_j\{\chi_i^*(\mathbf{r}_1)\chi_j\ (\mathbf{r}_1)\chi_j^*(\mathbf{r}_2)\chi_i\ (\mathbf{r}_2)\}\right| \\ &= 2\left|-\sum_{ij} S_{ij}^{\mathrm{A}} S_{ji}^{\mathrm{B}}\right| \end{aligned} \tag{9}$$

where we have used the definition for the elements of the AOM from Eq. 7. δ(A,B) is known as the delocalization index (DI)[10,11] for atom pair A,B. In single-determinant wavefunctions, it is

often calculated by only considering spin-orbitals between parallel spin electrons, in order to calculate only the delocalization arising from Fermi correlation. Finally, note that the integrations can be swapped ($d\mathbf{r_1}$ over Ω(B), $d\mathbf{r_2}$ over Ω(A)) which will give the equivalent number of electrons, indicating that the number of electrons found on average in Ω(A) but delocalized into Ω(B) is the same as the number of electrons found on average in Ω(B) but delocalized into Ω(A); hence, the factor of 2 in Eq. 9.

Since Eq. 9 is written in terms of MOs, it is easy to recover the contribution of each MO and MO-pair to the total DI. A delocalized density matrix can be easily defined in terms of AOM elements:

$$D_{ij}^{(\mathrm{A,B})} = 2\left|-S_{ij}^{\mathrm{A}}S_{ji}^{\mathrm{B}}\right| \tag{10}$$

Diagonal elements of this matrix, $D_{ii}^{(\mathrm{A,B})}$, provides the contributions of each MO's contribution to the total number of electron pairs shared between A and B. However, the off-diagonal elements, $D_{i\neq j}^{(\mathrm{A,B})}$, provides the extent to which an MO-pair increases delocalized electron pairs (through constructive interference) or decreases delocalized electron pairs (through deconstructive interference). Therefore, the sum of any row or column of $\mathbf{D}_{ij}$ gives the net contribution of an MO to the number of electron pairs shared between atoms A and B, after any MO-pair interference effects have been taken into account.

MO	**MO 1**	**MO 2**	**MO 3**	**MO 4**	**MO 5**	**MO 6**	**MO 7**
MO 1	*1.00*	-1.00	0.00	0.00	0.00	0.00	0.00
MO 2	-1.00	*1.00*	0.00	0.00	0.00	0.00	0.00
MO 3	0.00	0.00	*1.00*	-0.27	0.00	0.00	0.00
MO 4	0.00	0.00	-0.27	*1.00*	-0.71	0.00	0.00
MO 5	0.00	0.00	0.00	-0.71	*1.00*	0.00	0.00
MO 6	0.00	0.00	0.00	0.00	0.00	*1.00*	0.00
MO 7	0.00	0.00	0.00	0.00	0.00	0.00	*1.00*
Sum	0.00	0.00	0.73	0.02	0.29	1.00	1.00
Percentage	0%	0%	24%	1%	10%	33%	33%

Figure S1. Delocalized matrix for N_2, as calculated at HF/6-311++G(2df,2pd) level.

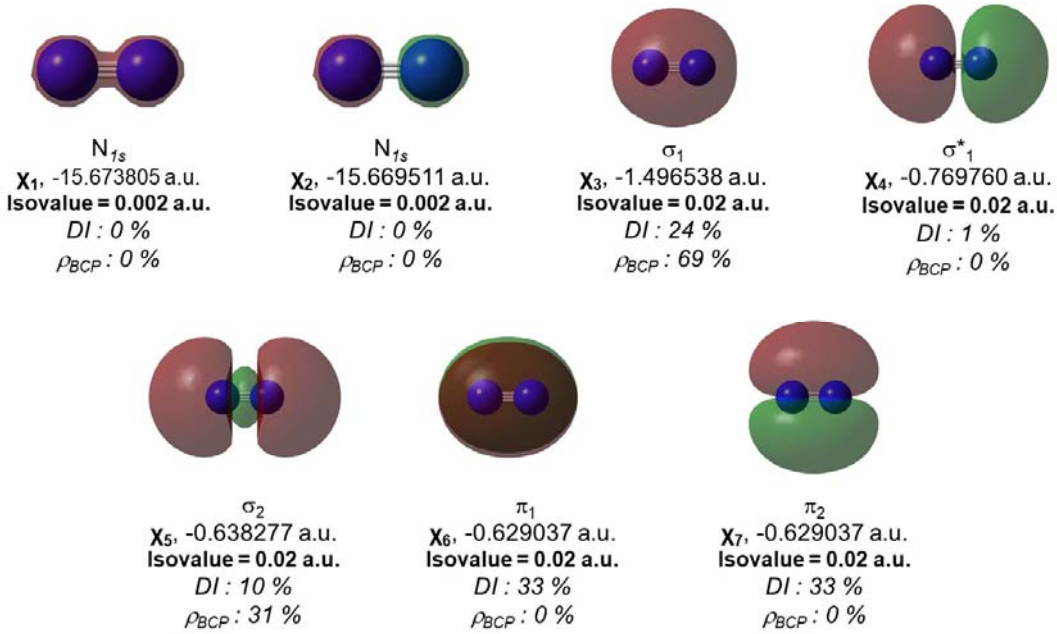

Figure S2. 3D-isosurfaces of MOs of N_2 at the HF/6-311++g(2df,2pd) level. Percentage **c**ontributions to the *DI*(N,N) as well as to the electron density at the (3,–1) CP(N,N) are also shown.

For instance, consider the MOs in N_2, as calculated by HF/6-311++G(2df,2pd), shown in Figure S2. The delocalized matrix **D** is shown above, in Figure S1. The core $1s_N$ orbitals form a bonding and antibonding pair, χ_1 and χ_2. Both MOs contribute 1 electron pair to the total DI ($D_{11}^{(A,B)} = D_{22}^{(A,B)} = 1.0$). However, the two orbitals are out-of-phase with each other, and interferes destructively so that $D_{12}^{(A,B)} = D_{21}^{(A,B)} = -1.0$. Therefore, the net contribution of MOs 1 and 2 is 0 electron pairs each, showing a classical bonding-antibonding pair. However, χ_3 – a σ-bonding MO – also contributes 1.0 electron pairs to the total DI, but interferes only weakly with χ_4 – a σ-antibonding MO. The net contribution of χ_3 is then 0.72 electron pairs. Finally, χ_4 interferes deconstructively with both χ_3 and χ_5 (the second σ-bonding MO), thereby bringing its net contribution down to only 0.02 electron pairs.

References

1. R. F. Bader. In *Atoms in molecules*; Wiley Online Library, **1990**.
2. S. Shahbazian. *Chem. Eur. J.* **2018**, *doi*: 10.1002/chem.201705163.

3. J. Contreras-García; E. R. Johnson; S. Keinan; R. Chaudret; J.-P. Piquemal; D. N. Beratan; W. Yang. *J. Chem. Theory Comput.* **2011**, *7*, 625-632.
4. A. Otero-de-la-Roza; E. R. Johnson; J. Contreras-García. *PCCP* **2012**, *14*, 12165-12172.
5. I. Cukrowski; J. H. de Lange; A. S. Adeyinka; P. Mangondo. *Comput. Theor. Chem.* **2015**, *1053*, 60-76.
6. J. H. de Lange; D. M. van Niekerk; I. Cukrowski. *J. Comput. Chem.* **2018**, *39*, 973-985.
7. J. H. Lange; I. Cukrowski. *J. Comput. Chem.* **2017**, *38*, 981-997.
8. R. F. Bader. *Monatshefte für Chemie/Chemical Monthly* **2005**, *136*, 819-854.
9. F. Cortés-Guzmán; R. F. Bader. *Coord. Chem. Rev.* **2005**, *249*, 633-662.
10. R. F. Bader; M. E. Stephens. *J. Am. Chem. Soc.* **1975**, *97*, 7391-7399.
11. R. Daudel; R. Bader; M. Stephens; D. Borrett. *Can. J. Chem.* **1974**, *52*, 1310-1320.

End of Part 1

Part 2. Cartesian coordinates of molecules studied

Table S1. Cartesian coordinates of planar biphenyl at the B3LYP/6-311++g(2df,2pd)/GD3 level.

Atom	X	Y	Z
C1	0.000000	0.745401	0.000000
C2	1.194303	1.480695	0.000000
C3	1.196327	2.868658	0.000000
C4	0.000000	3.575187	0.000000
C5	-1.196327	2.868658	0.000000
C6	-1.194303	1.480695	0.000000
H7	2.147022	0.973835	0.000000
H8	2.139620	3.398460	0.000000
H9	0.000000	4.656587	0.000000
H10	-2.139620	3.398460	0.000000
H11	-2.147022	0.973835	0.000000
C12	0.000000	-0.745401	0.000000
C13	-1.194303	-1.480695	0.000000
C14	1.194303	-1.480695	0.000000
C15	-1.196327	-2.868658	0.000000
H16	-2.147022	-0.973835	0.000000
C17	1.196327	-2.868658	0.000000
H18	2.147022	-0.973835	0.000000
C19	0.000000	-3.575187	0.000000
H20	-2.139620	-3.398460	0.000000
H21	2.139620	-3.398460	0.000000
H22	0.000000	-4.656587	0.000000

Table S2. Cartesian coordinates of twisted biphenyl at the B3LYP/6-311++g(2df,2pd)/GD3 level.

Atom	X	Y	Z
C1	0.000000	0.740639	0.000000
C2	1.125949	1.459671	0.416302
C3	1.126421	2.848508	0.416623
C4	0.000000	3.549616	0.000000
C5	-1.126421	2.848508	-0.416623
C6	-1.125949	1.459671	-0.416302
H7	1.999325	0.924884	0.764579
H8	2.005079	3.383880	0.751032
H9	0.000000	4.631157	0.000000
H10	-2.005079	3.383880	-0.751032
H11	-1.999325	0.924884	-0.764579
C12	0.000000	-0.740639	0.000000
C13	-1.125949	-1.459671	0.416302
C14	1.125949	-1.459671	-0.416302
C15	-1.126421	-2.848508	0.416623
H16	-1.999325	-0.924884	0.764579
C17	1.126421	-2.848508	-0.416623
H18	1.999325	-0.924884	-0.764579
C19	0.000000	-3.549616	0.000000
H20	-2.005079	-3.383880	0.751032
H21	2.005079	-3.383880	-0.751032
H22	0.000000	-4.631157	0.000000

Table S3. Cartesian coordinates of cubic Li_4H_4 at the B3LYP/6-311++g(2df,2pd)/GD3 level.

Atom	X	Y	Z
Li1	-1.118656	-0.942737	-0.365387
H2	-1.449309	0.667838	0.437822
Li3	-0.189314	1.309120	-0.723882
H4	0.013932	-0.265758	-1.633203
H5	0.207746	-1.436650	0.794396
Li6	-0.012695	0.242165	1.488227
H7	1.227625	1.034573	0.400985
Li8	1.320666	-0.608549	-0.398958

End of Part 2

Part 3 – Canonical molecular orbitals in biphenyl

Table S4. Full list of MOs in the planar Bph; isovalue = 0.01 a.u.

MO	Top View	Side View
χ_1	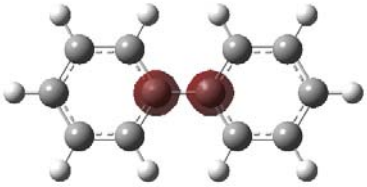	
χ_2	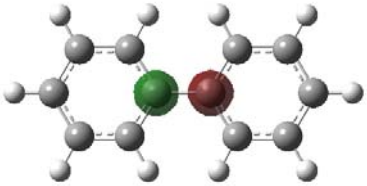	
χ_3	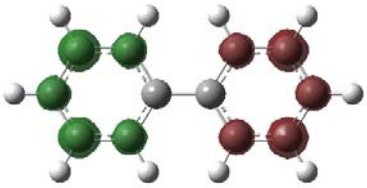	
χ_4	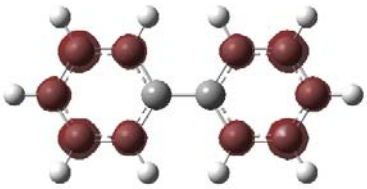	
χ_5	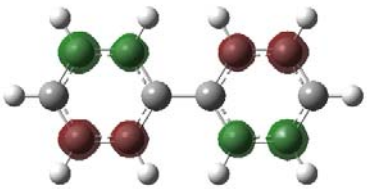	
χ_6	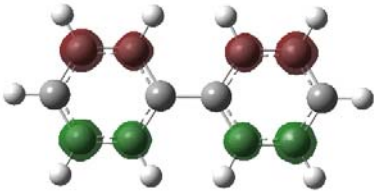	

Table S4 continues – planar Bph.

χ_7	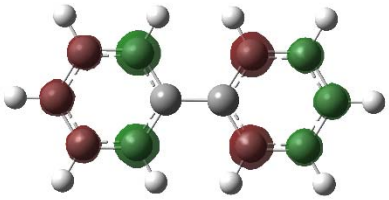	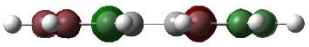
χ_8	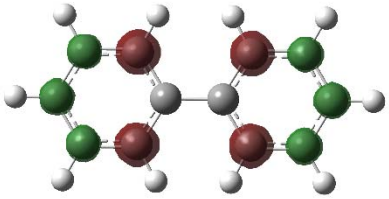	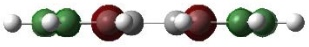
χ_9	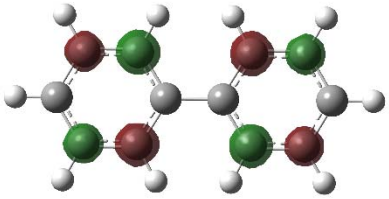	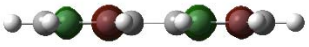
χ_{10}	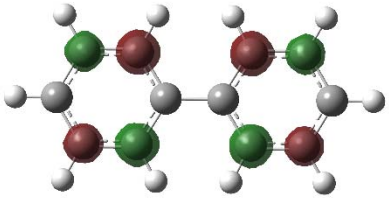	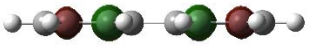
χ_{11}	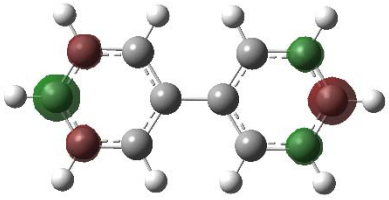	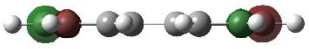
χ_{12}	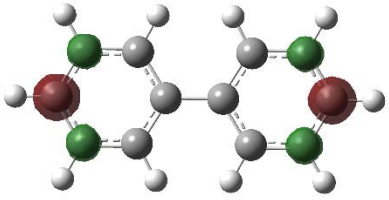	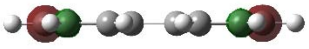

Table S4 continues – planar Bph.

χ_{13}	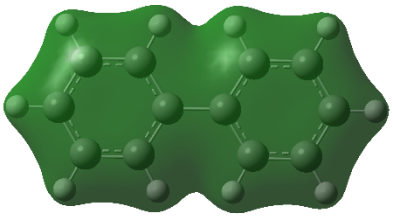	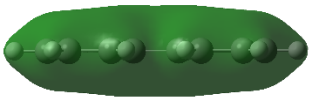
χ_{14}	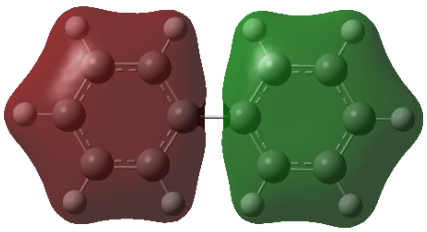	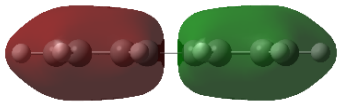
χ_{15}	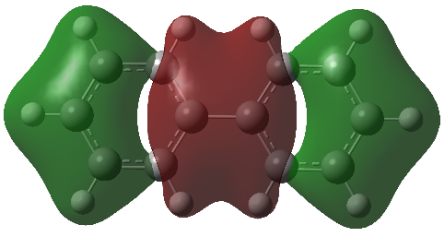	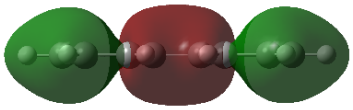
χ_{16}	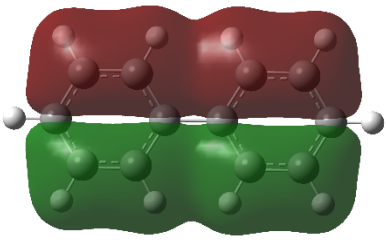	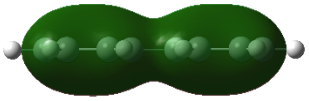
χ_{17}	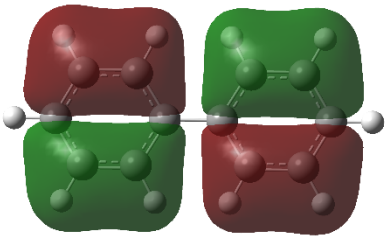	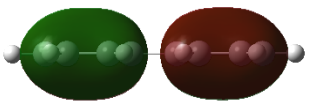
χ_{18}	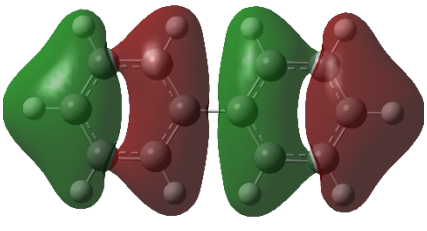	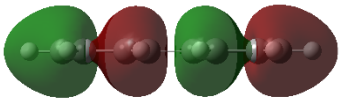

Table S4 continues – planar Bph.

χ_{19}	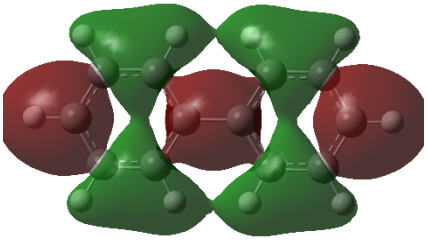	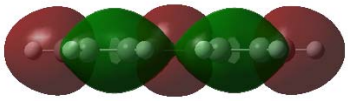
χ_{20}	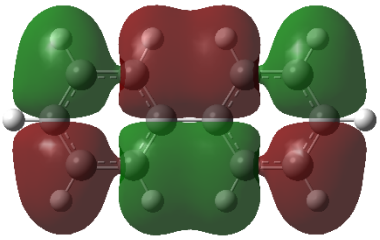	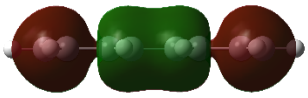
χ_{21}	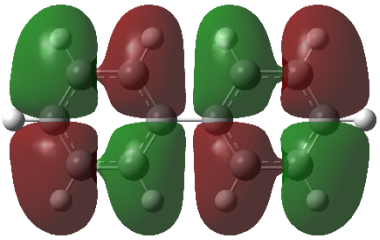	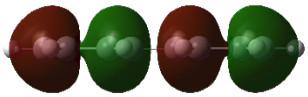
χ_{22}	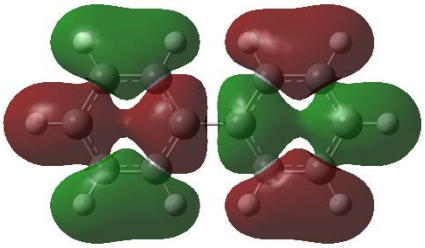	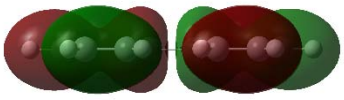
χ_{23}	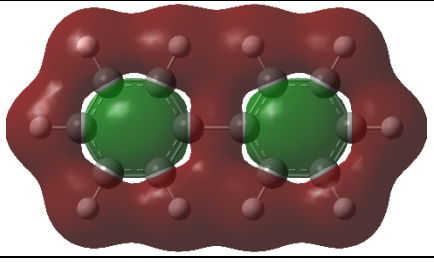	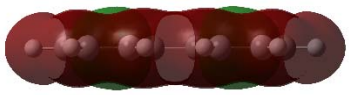
χ_{24}	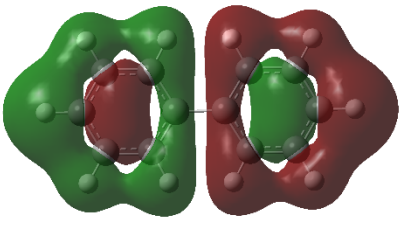	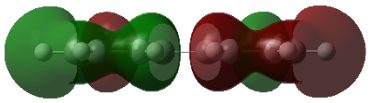

Table S4 continues – planar Bph.

χ_{25}	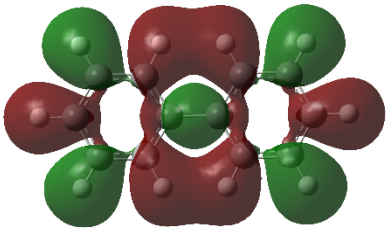	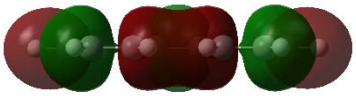
χ_{26}	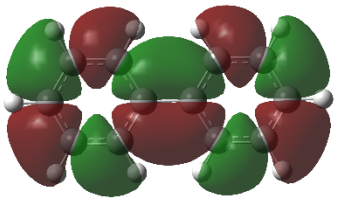	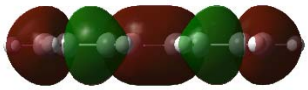
χ_{27}	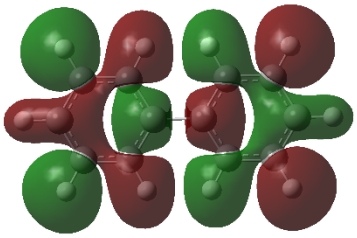	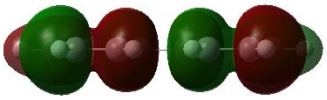
χ_{28}	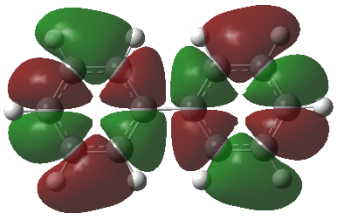	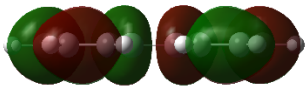
χ_{29}	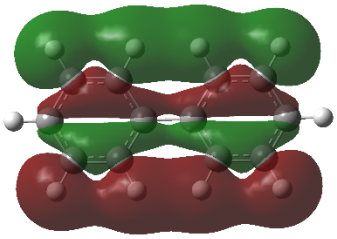	
χ_{30}	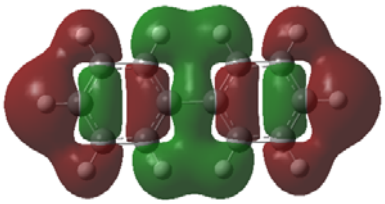	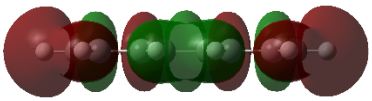

Table S4 continues – planar Bph.

χ_{31}	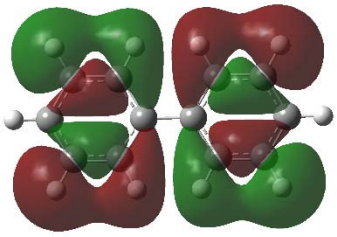	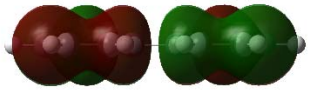
χ_{32}	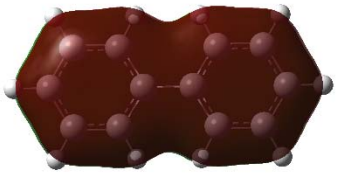	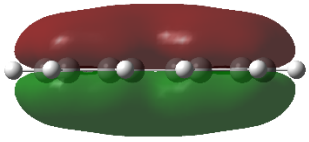
χ_{33}	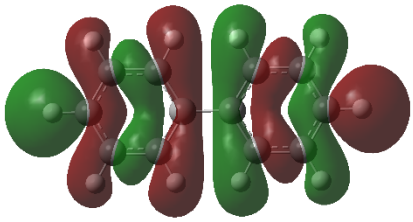	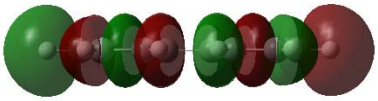
χ_{34}	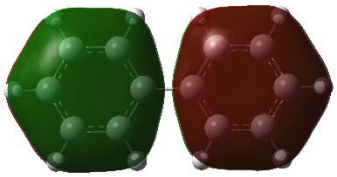	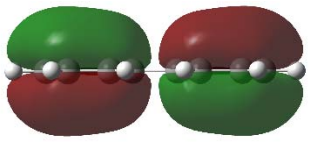
χ_{35}	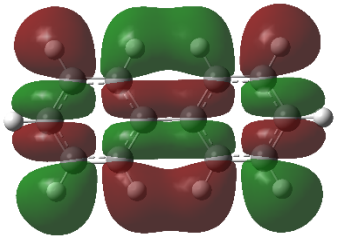	
χ_{36}	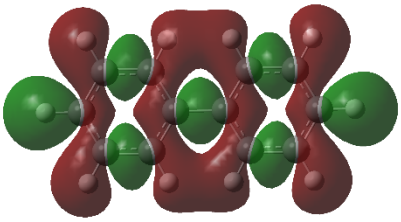	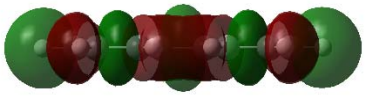

Table S4 continues – planar Bph.

χ_{37}	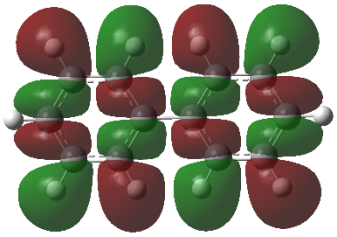	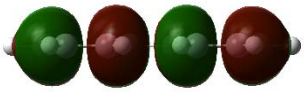
χ_{38}	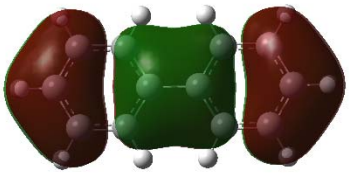	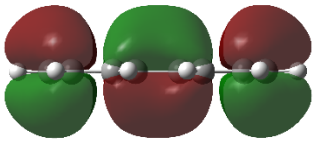
χ_{39}	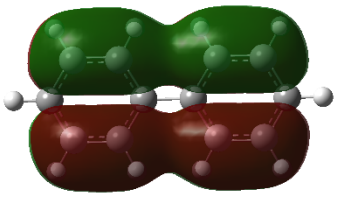	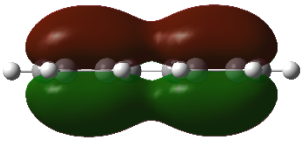
χ_{40}	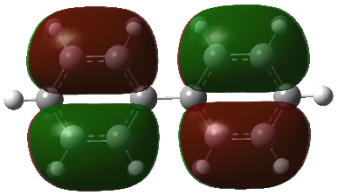	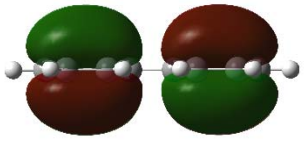
χ_{41}	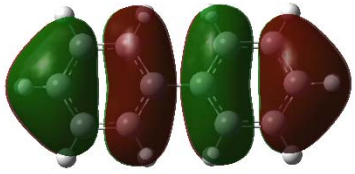	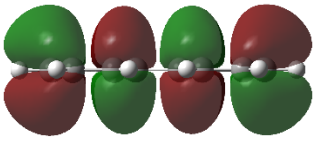

Table S5. Full list of MOs in the twisted Bph; isovalue = 0.01 a.u.

MO	Top View	Side View
χ_1	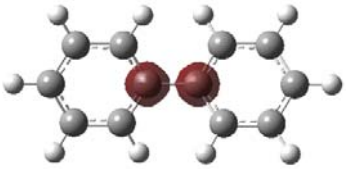	
χ_2	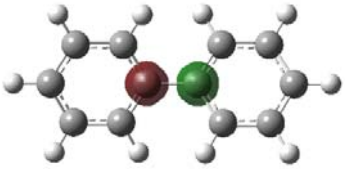	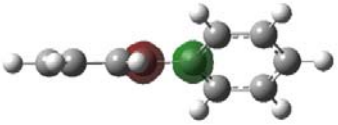
χ_3	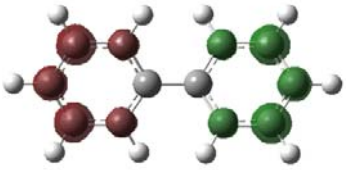	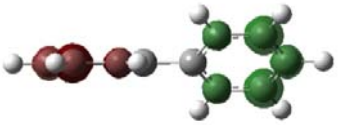
χ_4	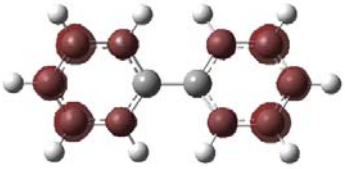	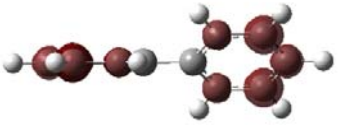
χ_5	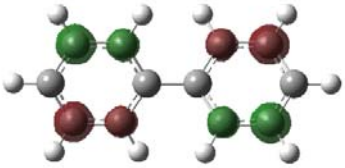	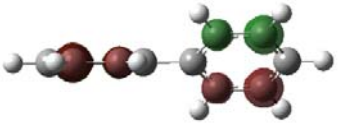
χ_6	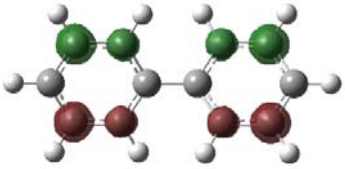	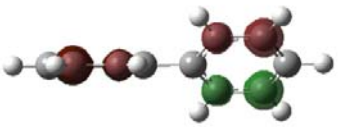

Table S5 continues – twisted Bph.

χ_7	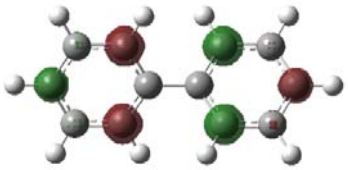	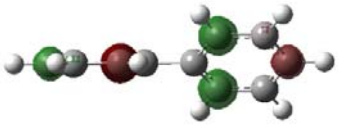
χ_8	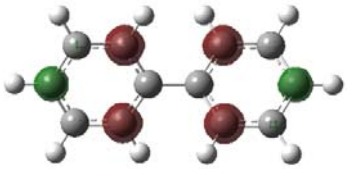	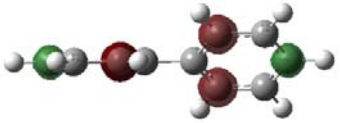
χ_9	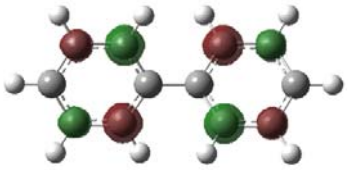	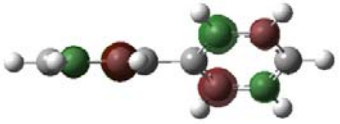
χ_{10}	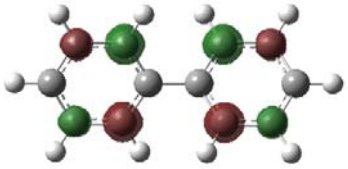	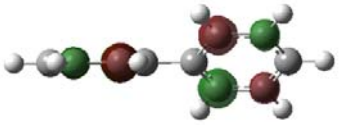
χ_{11}	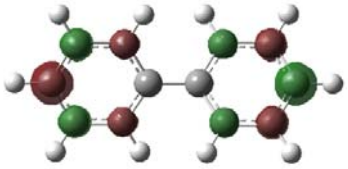	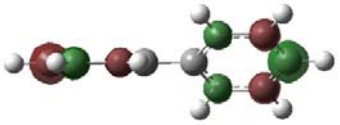
χ_{12}	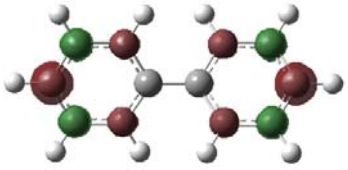	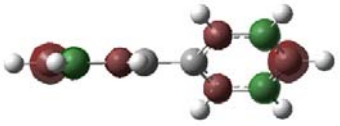

Table S5 continues – twisted Bph.

χ_{13}	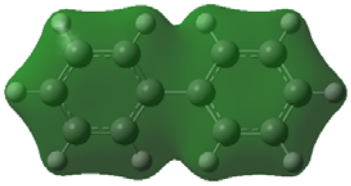	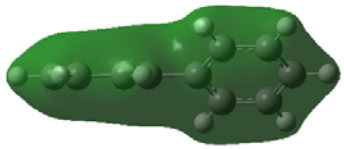
χ_{14}	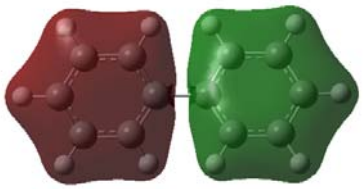	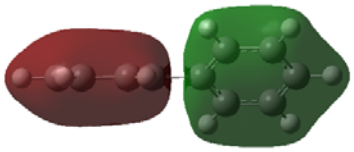
χ_{15}	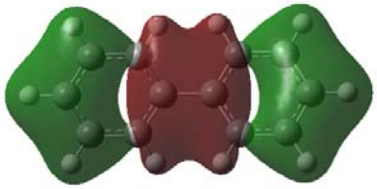	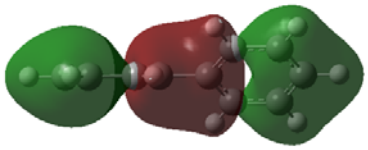
χ_{16}	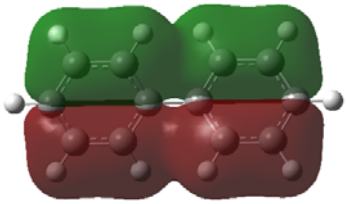	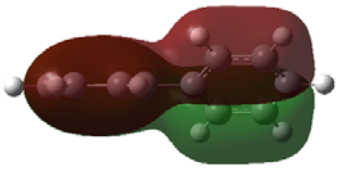
χ_{17}	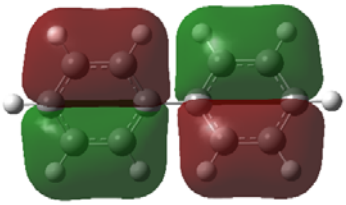	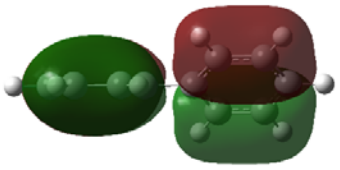
χ_{18}	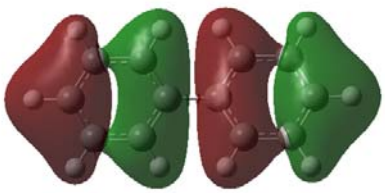	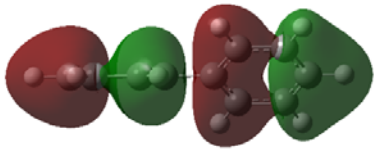

Table S5 continues – twisted Bph.

χ_{19}	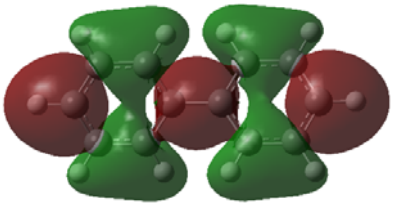	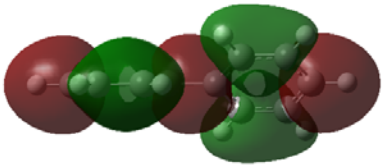
χ_{20}	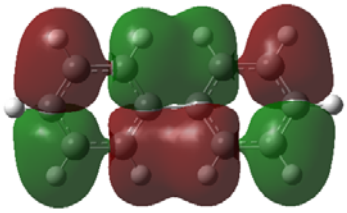	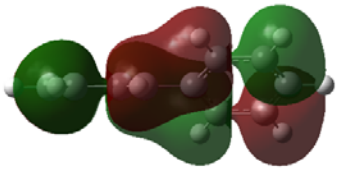
χ_{21}	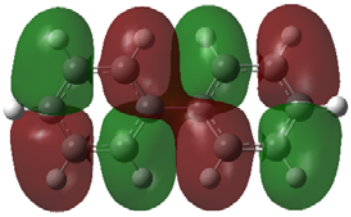	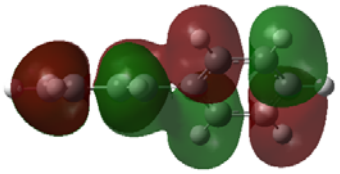
χ_{22}	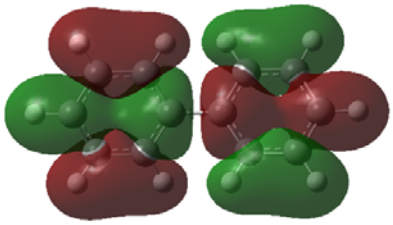	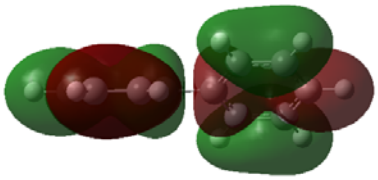
χ_{23}	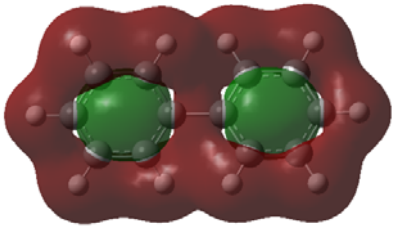	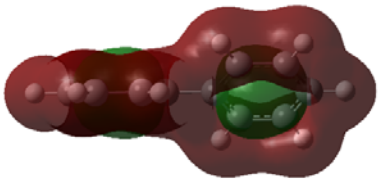
χ_{24}	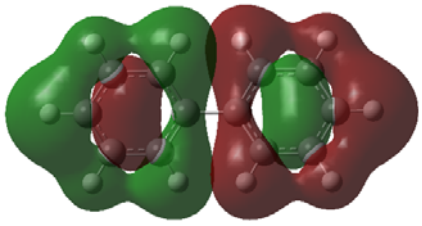	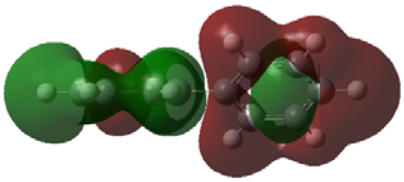

Table S5 continues – twisted Bph.

χ_{25}	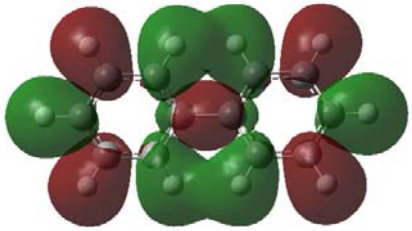	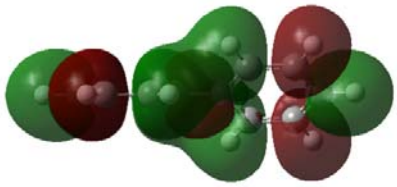
χ_{26}	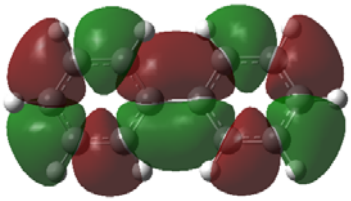	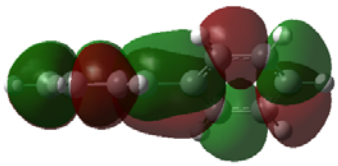
χ_{27}	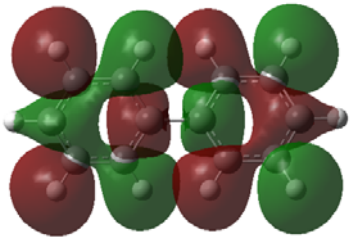	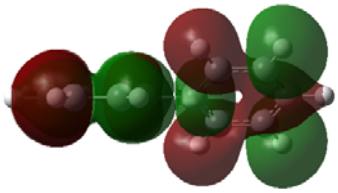
χ_{28}	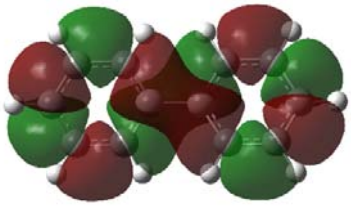	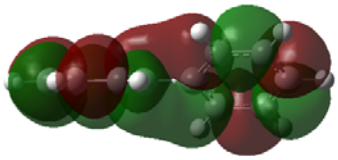
χ_{29}	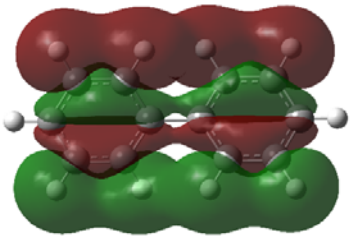	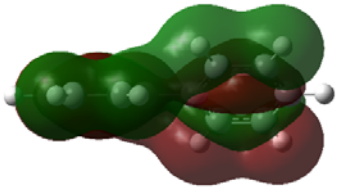
χ_{30}	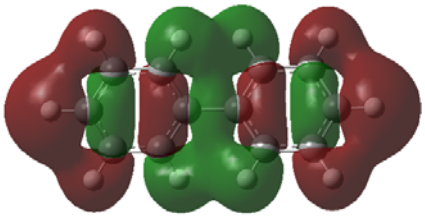	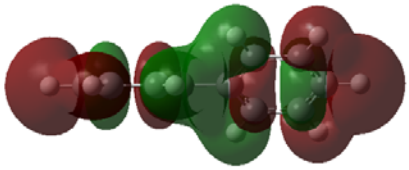

Table S5 continues – twisted Bph.

χ_{31}	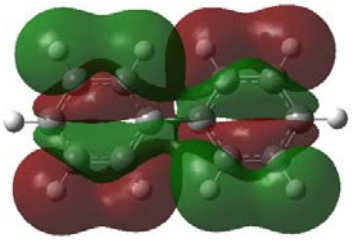	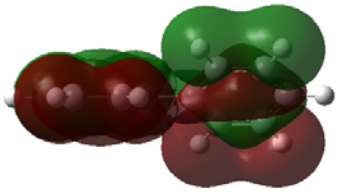
χ_{32}	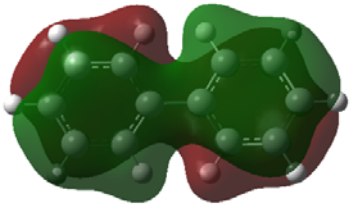	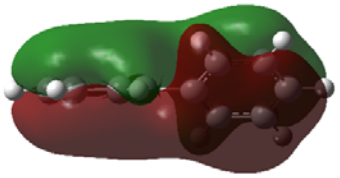
χ_{33}	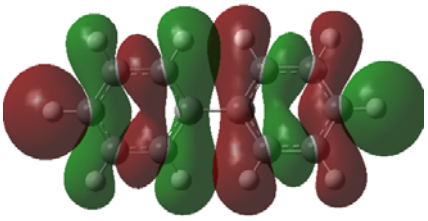	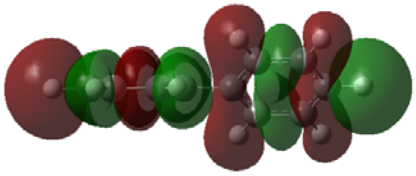
χ_{34}	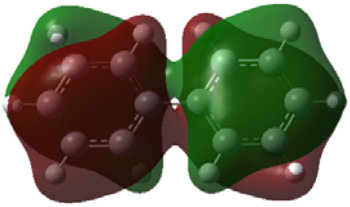	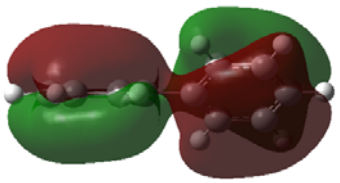
χ_{35}	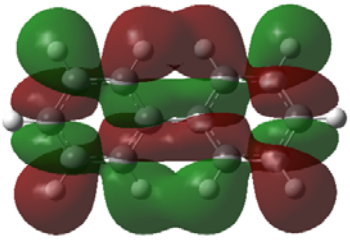	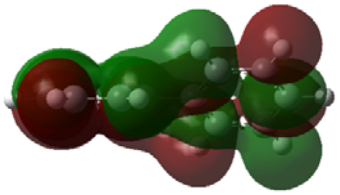
χ_{36}	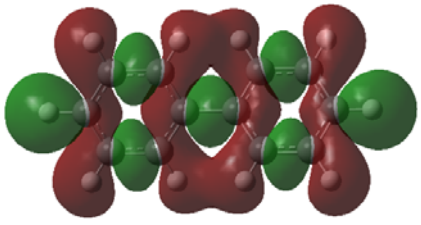	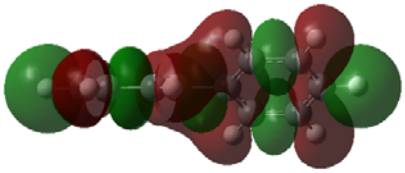

Table S5 continues – twisted Bph.

χ_{37}	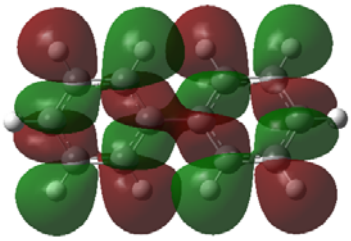	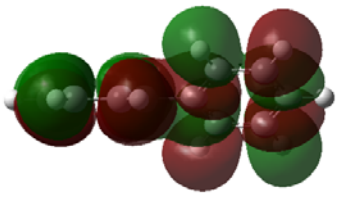
χ_{38}	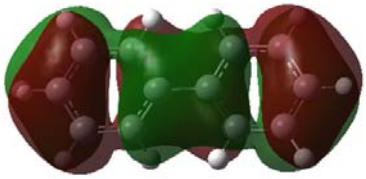	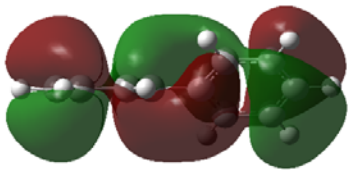
χ_{39}	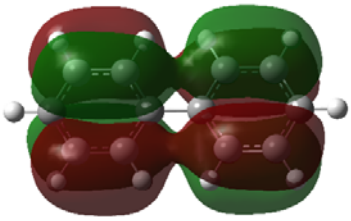	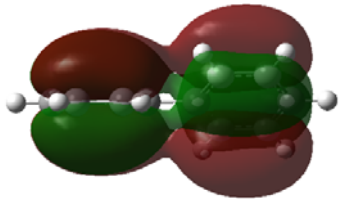
χ_{40}	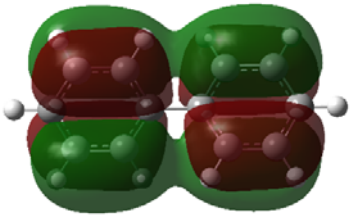	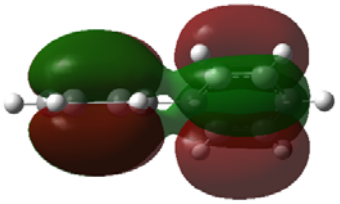
χ_{41}	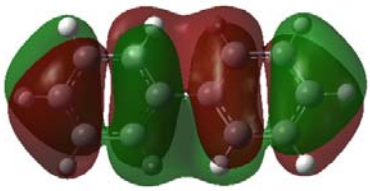	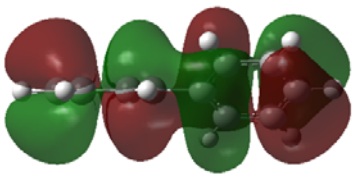

End of Part 3

Part 4 – Data pertaining to covalent bonds in biphenyl

Table S6. MO-ED data at (3,–1) CP(C1,C12) & CP(C19,H22) in the planar Bph.

		C1,C12		C19,H22	
MO	Energy (a.u.)	ED contribution (a.u.) / %-fraction	Classification based on 2nd derivative sign (λ_2)	ED contribution (a.u.) / %-fraction	Classification based on 2nd derivative sign (λ_2)
χ_1	-10.19173	0.00010 / 0.0%	*concentrating*	0.00000 / 0.0%	*non-contributing*
χ_2	-10.19145	0.00000 / 0.0%	*non-contributing*	0.00000 / 0.0%	*non-contributing*
χ_3	-10.17726	0.00000 / 0.0%	*non-contributing*	0.00000 / 0.0%	*non-contributing*
χ_4	-10.17724	0.00000 / 0.0%	*non-contributing*	0.00000 / 0.0%	*non-contributing*
χ_5	-10.17720	0.00000 / 0.0%	*non-contributing*	0.00000 / 0.0%	*non-contributing*
χ_6	-10.17718	0.00000 / 0.0%	*non-contributing*	0.00000 / 0.0%	*non-contributing*
χ_7	-10.17658	0.00000 / 0.0%	*non-contributing*	0.00000 / 0.0%	*non-contributing*
χ_8	-10.17657	0.00000 / 0.0%	*non-contributing*	0.00000 / 0.0%	*non-contributing*
χ_9	-10.17653	0.00000 / 0.0%	*non-contributing*	0.00000 / 0.0%	*non-contributing*
χ_{10}	-10.17652	0.00000 / 0.0%	*non-contributing*	0.00000 / 0.0%	*non-contributing*
χ_{11}	-10.17586	0.00000 / 0.0%	*non-contributing*	0.00005 / 0.0%	*concentrating*
χ_{12}	-10.17586	0.00000 / 0.0%	*non-contributing*	0.00005 / 0.0%	*concentrating*
χ_{13}	-0.87581	0.01896 / 7.2%	*concentrating*	0.00150 / 0.5%	*concentrating*
χ_{14}	-0.85459	0.00000 / 0.0%	*non-contributing*	0.00357 1.2%	*concentrating*
χ_{15}	-0.78384	0.03774 / 14.3%	*concentrating*	0.00980 / 3.3%	*concentrating*
χ_{16}	-0.75827	0.00000 / 0.0%	*non-contributing*	0.00000 / 0.0%	*non-contributing*
χ_{17}	-0.74841	0.00000 / 0.0%	*non-contributing*	0.00000 / 0.0%	*non-contributing*
χ_{18}	-0.72791	0.00000 / 0.0%	*non-contributing*	0.01662 / 5.7%	*concentrating*
χ_{19}	-0.63238	0.04513 / 17.1%	*concentrating*	0.02476 / 8.5%	*concentrating*
χ_{20}	-0.62793	0.00000 / 0.0%	*non-contributing*	0.00000 / 0.0%	*non-contributing*
χ_{21}	-0.59212	0.00000 / 0.0%	*non-contributing*	0.00000 / 0.0%	*non-contributing*
χ_{22}	-0.58592	0.00000 / 0.0%	*non-contributing*	0.01386 / 4.7%	*concentrating*
χ_{23}	-0.54310	0.01894 / 7.2%	*concentrating*	0.01360 4.6%	*concentrating*
χ_{24}	-0.50360	0.00000 / 0.0%	*non-contributing*	0.05810 / 19.9%	*concentrating*
χ_{25}	-0.48074	0.03774 / 14.3%	*concentrating*	0.02312 / 7.9%	*concentrating*
χ_{26}	-0.47350	0.00000 / 0.0%	*non-contributing*	0.00000 / 0.0%	*non-contributing*
χ_{27}	-0.44376	0.00000 / 0.0%	*non-contributing*	0.00263 / 0.9%	*concentrating*
χ_{28}	-0.43615	0.00000 / 0.0%	*non-contributing*	0.00000 / 0.0%	*non-contributing*
χ_{29}	-0.43567	0.00000 / 0.0%	*non-contributing*	0.00000 / 0.0%	*non-contributing*
χ_{30}	-0.43051	0.04133 / 15.6%	*concentrating*	0.04914 / 16.8%	*concentrating*

Table S6 continues.

		C1,C12		C19,H22	
MO	Energy (a.u.)	ED contribution (a.u.) / %-fraction	Classification based on 2nd derivative sign (λ_2)	ED contribution (a.u.) / %-fraction	Classification based on 2nd derivative sign (λ_2)
χ_{31}	-0.41671	0.00000 / 0.0%	*non-contributing*	0.00000 / 0.0%	*non-contributing*
χ_{32}	-0.39513	0.00000 / 0.0%	*depleting*	0.00000 / 0.0%	*depleting*
χ_{33}	-0.36916	0.00000 / 0.0%	*non-contributing*	0.05161 / 17.6%	*concentrating*
χ_{34}	-0.36616	0.00000 / 0.0%	*non-contributing*	0.00000 / 0.0%	*depleting*
χ_{35}	-0.36285	0.00000 / 0.0%	*non-contributing*	0.00000 / 0.0%	*non-contributing*
χ_{36}	-0.34790	0.06432 / 24.3%	*concentrating*	0.02425 / 8.3%	*concentrating*
χ_{37}	-0.33466	0.00000 / 0.0%	*non-contributing*	0.00000 / 0.0%	*non-contributing*
χ_{38}	-0.29363	0.00000 / 0.0%	*depleting*	0.00000 / 0.0%	*depleting*
χ_{39}	-0.26531	0.00000 / 0.0%	*non-contributing*	0.00000 / 0.0%	*non-contributing*
χ_{40}	-0.25903	0.00000 / 0.0%	*non-contributing*	0.00000 / 0.0%	*non-contributing*
χ_{41}	-0.23027	0.00000 / 0.0%	*non-contributing*	0.00000 / 0.0%	*depleting*

Table S7. MO-DI data (in e^--pairs) for covalent bond C1–C12 in the planar Bph.

MO	1–21[a]	22	23	24	25	26	27	28	29	30	31	32	33	34	35	36	37	38	39	40	41
1–21	0.38[a]	-0.02	0.00	-0.01	0.05	0.02	-0.01	-0.01	0.00	0.00	0.00	0.00	-0.01	0.00	0.01	0.02	-0.01	0.00	0.00	0.00	0.00
22	-0.02	0.02	0.00	0.00	0.00	0.00	0.01	0.00	0.00	-0.01	0.00	0.00	0.00	0.00	0.00	0.00	0.00	0.00	0.00	0.00	0.00
23	0.00	0.00	0.02	0.00	0.01	0.00	0.00	0.00	0.00	0.03	0.00	0.00	0.00	0.00	0.00	0.03	0.00	0.00	0.00	0.00	0.00
24	-0.01	0.00	0.00	0.00	0.00	0.00	0.00	0.00	0.00	0.00	0.00	0.00	0.00	0.00	0.00	0.00	0.00	0.00	0.00	0.00	0.00
25	0.05	0.00	0.01	0.00	0.01	0.00	0.00	0.00	0.00	0.01	0.00	0.00	0.00	0.00	0.00	0.02	0.00	0.00	0.00	0.00	0.00
26	0.02	0.00	0.00	0.00	0.00	0.03	0.00	-0.02	0.00	0.00	0.00	0.00	0.00	0.00	0.02	0.00	-0.02	0.00	0.00	0.00	0.00
27	-0.01	0.01	0.00	0.00	0.00	0.00	0.01	0.00	0.00	0.00	0.00	0.00	0.00	0.00	0.00	0.00	0.00	0.00	0.00	0.00	0.00
28	-0.01	0.00	0.00	0.00	0.00	-0.02	0.00	0.03	-0.01	0.00	0.00	0.00	0.00	0.00	-0.01	0.00	0.02	0.00	0.00	0.00	0.00
29	0.00	0.00	0.00	0.00	0.00	0.00	0.00	-0.01	0.00	0.00	0.00	0.00	0.00	0.00	0.00	0.00	-0.01	0.00	0.00	0.00	0.00
30	0.00	-0.01	0.03	0.00	0.01	0.00	0.00	0.00	0.00	0.05	0.00	0.00	0.00	0.00	0.00	0.05	0.00	0.00	0.00	0.00	0.00
31	0.00	0.00	0.00	0.00	0.00	0.00	0.00	0.00	0.00	0.00	0.00	0.00	0.00	0.00	0.00	0.00	0.00	0.00	0.00	0.00	0.00
32	0.00	0.00	0.00	0.00	0.00	0.00	0.00	0.00	0.00	0.00	0.00	0.11	0.00	-0.02	0.00	0.00	0.00	0.09	0.00	0.00	-0.07
33	-0.01	0.00	0.00	0.00	0.00	0.00	0.00	0.00	0.00	0.00	0.00	0.00	0.00	0.00	0.00	0.00	0.00	0.00	0.00	0.00	0.00
34	0.00	0.00	0.00	0.00	0.00	0.00	0.00	0.00	0.00	0.00	0.00	-0.02	0.00	0.01	0.00	0.00	0.00	-0.02	0.00	0.00	0.02
35	0.01	0.00	0.00	0.00	0.00	0.02	0.00	-0.01	0.00	0.00	0.00	0.00	0.00	0.00	0.01	0.00	-0.01	0.00	0.00	0.00	0.00
36	0.02	0.00	0.03	0.00	0.02	0.00	0.00	0.00	0.00	0.05	0.00	0.00	0.00	0.00	0.00	0.05	0.00	0.00	0.00	0.00	0.00
37	-0.01	0.00	0.00	0.00	0.00	-0.02	0.00	0.02	-0.01	0.00	0.00	0.00	0.00	0.00	-0.01	0.00	0.02	0.00	0.00	0.00	0.00
38	0.00	0.00	0.00	0.00	0.00	0.00	0.00	0.00	0.00	0.00	0.00	0.09	0.00	-0.02	0.00	0.00	0.00	0.08	0.00	0.00	-0.06
39	0.00	0.00	0.00	0.00	0.00	0.00	0.00	0.00	0.00	0.00	0.00	0.00	0.00	0.00	0.00	0.00	0.00	0.00	0.00	0.00	0.00
40	0.00	0.00	0.00	0.00	0.00	0.00	0.00	0.00	0.00	0.00	0.00	0.00	0.00	0.00	0.00	0.00	0.00	0.00	0.00	0.00	0.00
41	0.00	0.00	0.00	0.00	0.00	0.00	0.00	0.00	0.00	0.00	0.00	-0.07	0.00	0.02	0.00	0.00	0.00	-0.06	0.00	0.00	0.06
Diagonal	2.30[a]	0.02	0.02	0.00	0.01	0.03	0.01	0.03	0.00	0.05	0.00	0.11	0.00	0.01	0.01	0.05	0.02	0.08	0.00	0.00	0.06
Off-Diagonal	-1.87[a]	-0.03	0.06	0.00	0.09	-0.01	0.00	-0.03	0.00	0.08	0.00	0.00	-0.01	-0.02	0.00	0.11	-0.03	0.01	0.00	0.00	-0.11
Total	0.43	0.00	0.08	0.00	0.11	0.02	0.00	-0.01	0.00	0.13	0.00	0.10	-0.01	-0.01	0.01	0.16	-0.01	0.10	0.00	0.00	-0.05

[a] MOs 1–21 were combined for the sake of brevity. The contributions made by diagonal elements of these MOs equal 2.30, whereas off-diagonal terms of only these MOs equal –1.92 to give a net contribution of 0.38. Interference with the remaining MOs (MOs 22–41) gives a positive, off-diagonal contribution of +0.05, so that the total contribution of MOs 1–21 equals 0.43.

Table S8. MO-DI data (in e^--pairs) for covalent bond C19–H22 in planar Bph.

MO	1–21[a]	22	23	24	25	26	27	28	29	30	31	32	33	34	35	36	37	38	39	40	41
1–21	0.13[a]	0.02	0.00	0.02	0.02	0.00	0.01	0.00	0.00	0.00	0.00	0.00	0.00	0.00	0.00	0.00	0.00	0.00	0.00	0.00	0.00
22	0.02	0.00	0.00	0.01	0.00	0.00	0.00	0.00	0.00	0.00	0.00	0.00	0.00	0.00	0.00	0.00	0.00	0.00	0.00	0.00	0.00
23	0.00	0.00	0.00	0.01	0.00	0.00	0.00	0.00	0.00	0.01	0.00	0.00	0.01	0.00	0.00	0.00	0.00	0.00	0.00	0.00	0.00
24	0.02	0.01	0.01	0.05	0.01	0.00	0.00	0.00	0.00	0.04	0.00	0.00	0.04	0.00	0.00	0.02	0.00	0.00	0.00	0.00	0.00
25	0.02	0.00	0.00	0.01	0.01	0.00	0.00	0.00	0.00	0.01	0.00	0.00	0.01	0.00	0.00	0.00	0.00	0.00	0.00	0.00	0.00
26	0.00	0.00	0.00	0.00	0.00	0.00	0.00	0.00	0.00	0.00	0.00	0.00	0.00	0.00	0.00	0.00	0.00	0.00	0.00	0.00	0.00
27	0.01	0.00	0.00	0.00	0.00	0.00	0.00	0.00	0.00	0.00	0.00	0.00	0.00	0.00	0.00	0.00	0.00	0.00	0.00	0.00	0.00
28	0.00	0.00	0.00	0.00	0.00	0.00	0.00	0.00	0.00	0.00	0.00	0.00	0.00	0.00	0.00	0.00	0.00	0.00	0.00	0.00	0.00
29	0.00	0.00	0.00	0.00	0.00	0.00	0.00	0.00	0.00	0.00	0.00	0.00	0.00	0.00	0.00	0.00	0.00	0.00	0.00	0.00	0.00
30	0.00	0.00	0.01	0.04	0.01	0.00	0.00	0.00	0.00	0.04	0.00	0.00	0.04	0.00	0.00	0.02	0.00	0.00	0.00	0.00	0.00
31	0.00	0.00	0.00	0.00	0.00	0.00	0.00	0.00	0.00	0.00	0.00	0.00	0.00	0.00	0.00	0.00	0.00	0.00	0.00	0.00	0.00
32	0.00	0.00	0.00	0.00	0.00	0.00	0.00	0.00	0.00	0.00	0.00	0.00	0.00	0.00	0.00	0.00	0.00	0.00	0.00	0.00	0.00
33	0.00	0.00	0.01	0.04	0.01	0.00	0.00	0.00	0.00	0.04	0.00	0.00	0.04	0.00	0.00	0.02	0.00	0.00	0.00	0.00	0.00
34	0.00	0.00	0.00	0.00	0.00	0.00	0.00	0.00	0.00	0.00	0.00	0.00	0.00	0.00	0.00	0.00	0.00	0.00	0.00	0.00	0.00
35	0.00	0.00	0.00	0.00	0.00	0.00	0.00	0.00	0.00	0.00	0.00	0.00	0.00	0.00	0.00	0.00	0.00	0.00	0.00	0.00	0.00
36	0.00	0.00	0.00	0.02	0.00	0.00	0.00	0.00	0.00	0.02	0.00	0.00	0.02	0.00	0.00	0.01	0.00	0.00	0.00	0.00	0.00
37	0.00	0.00	0.00	0.00	0.00	0.00	0.00	0.00	0.00	0.00	0.00	0.00	0.00	0.00	0.00	0.00	0.00	0.00	0.00	0.00	0.00
38	0.00	0.00	0.00	0.00	0.00	0.00	0.00	0.00	0.00	0.00	0.00	0.00	0.00	0.00	0.00	0.00	0.00	0.00	0.00	0.00	0.00
39	0.00	0.00	0.00	0.00	0.00	0.00	0.00	0.00	0.00	0.00	0.00	0.00	0.00	0.00	0.00	0.00	0.00	0.00	0.00	0.00	0.00
40	0.00	0.00	0.00	0.00	0.00	0.00	0.00	0.00	0.00	0.00	0.00	0.00	0.00	0.00	0.00	0.00	0.00	0.00	0.00	0.00	0.00
41	0.00	0.00	0.00	0.00	0.00	0.00	0.00	0.00	0.00	0.00	0.00	0.00	0.00	0.00	0.00	0.00	0.00	0.00	0.00	0.00	0.00
Diagonal	0.03[a]	0.00	0.00	0.05	0.01	0.00	0.00	0.00	0.00	0.04	0.00	0.00	0.04	0.00	0.00	0.01	0.00	0.00	0.00	0.00	0.00
Off-Diagonal	0.17[a]	0.04	0.05	0.15	0.06	0.00	0.00	0.00	0.00	0.11	0.00	0.00	0.11	0.00	0.00	0.06	0.00	0.01	0.00	0.00	0.01
Total	0.20[a]	0.04	0.05	0.19	0.07	0.00	0.01	0.00	0.00	0.16	0.00	0.00	0.15	0.01	0.00	0.06	0.00	0.01	0.00	0.00	0.01

[a] MOs 1–21 were combined for the sake of brevity. The contributions made by diagonal elements of these MOs equal 0.03, whereas off-diagonal terms of only these MOs equal +0.1 to give a net contribution of 0.13. Interference with the remaining MOs (MOs 22–41) gives a positive, off-diagonal contribution of +0.04, so that the total contribution of MOs 1–21 equals 0.20.

Table S9. Summary of MO-ED & MO-DI data, for covalent bonds C1,C12 & C19,H22 in planar BPh

	C1,C12		C19,H22	
Classification based on λ_2	**Number of MOs**	**Contribution to ρ(CP)[a]**	**Number of MOs**	**Contribution to ρ(CP)[a]**
Concentrating	8	0.264	15	0.293
Depleting	2	0.000	4	0.000
Non-contributing	31	0.000	22	0.000
Delocalization		**Contribution to DI[b]**		**Contribution to DI[b]**
Overlapping		2.82		0.19
Interference		-1.76		0.77
Net DI		1.06		0.97

[a] in a.u.; [b] in e^--pairs.

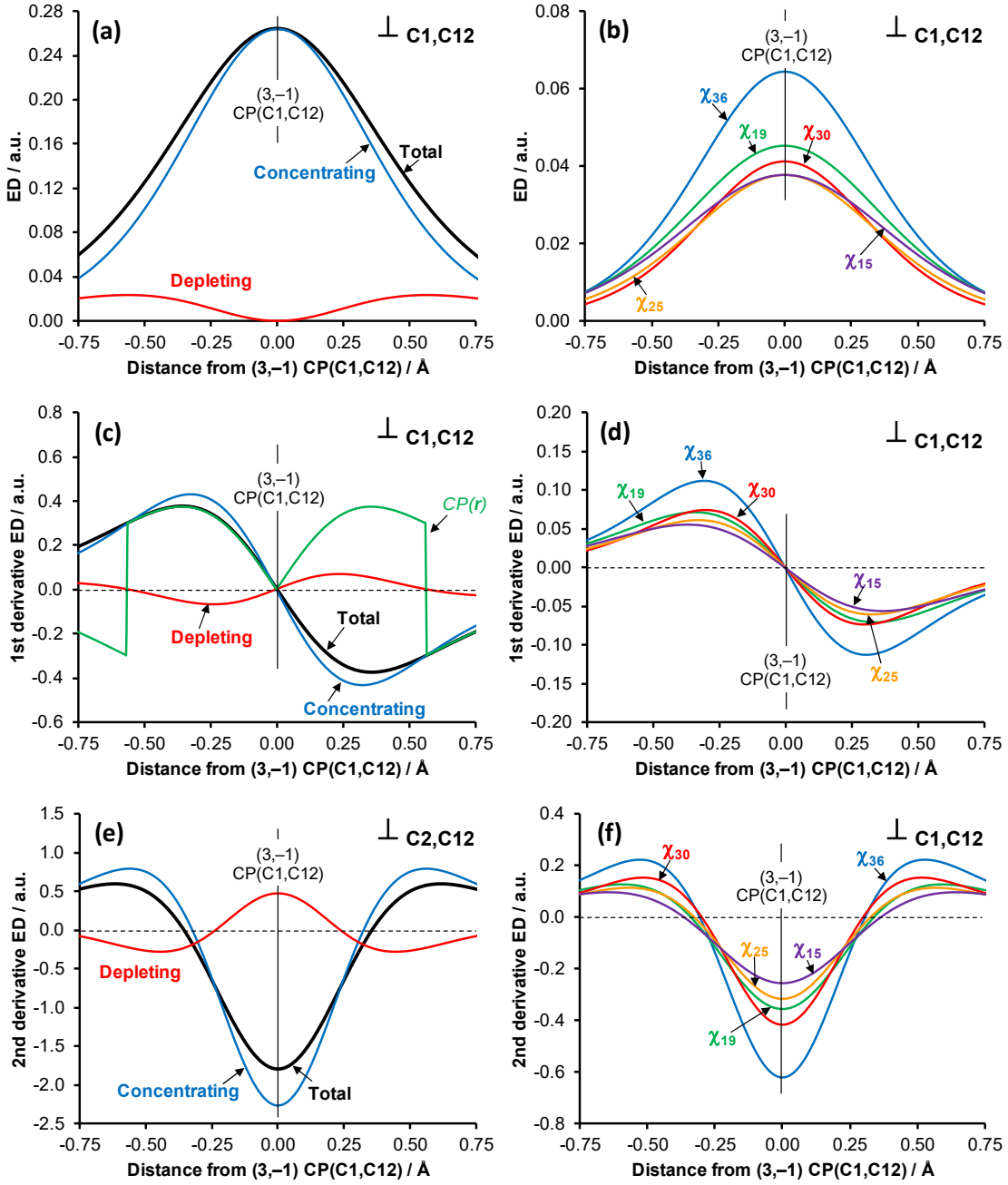

Figure S3. Decomposition of the total-ED (**a**), first derivative (**c**) and directional partial derivatives (**e**) along the λ_2–eigenvector in the C1,C12 inter-nuclear region in planar biphenyl, as well as the subsequent decomposition of the concentrating density into the largest MO contributions (**b,d,f)**

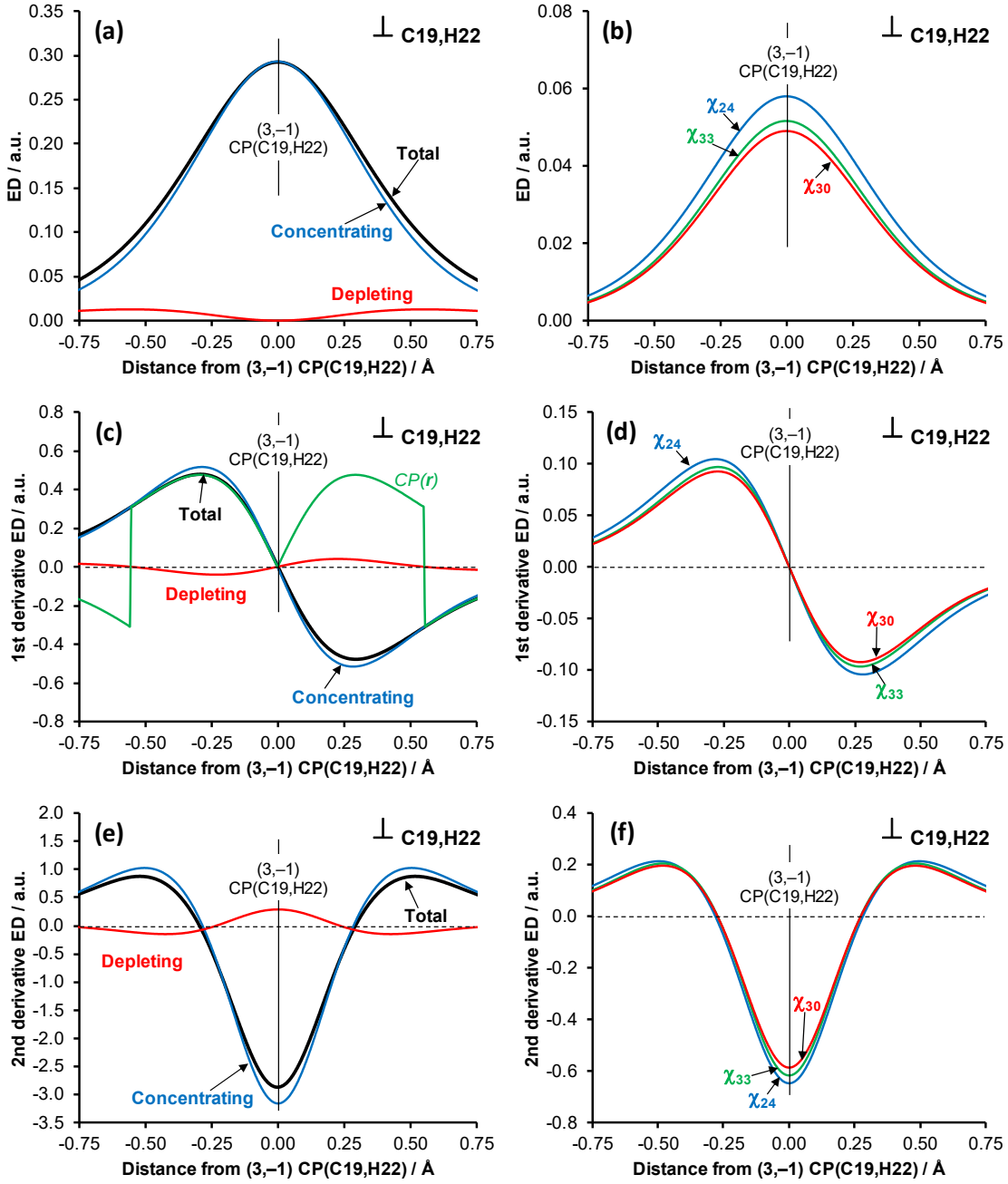

Figure S4. Decomposition of the total-ED (**a**), first derivative (**c**) and directional partial derivatives (**e**) along the λ_2–eigenvector in the C19,H22 inter-nuclear region in planar biphenyl, as well as the subsequent decomposition of the concentrating density into the largest MO contributions (**b,d,f)**

End of Part 4

Part 5 – Data pertaining to CP/MDP(H7,H18) in the planar/twisted biphenyl

Table S10. MO-ED data at (3,–1) CP(H7,H18) in planar and at MDP(H7,H18) in twisted Bph.

		Planar		**Twisted**	
MO	Energy (a.u.)	ED contribution (a.u.) / %-fraction	Classification based on 2nd derivative sign (λ_2)	ED contribution (a.u.) / %-fraction	Classification based on 2nd derivative sign (λ_2)
χ_1	-10.19173	0.00000 / 0.0%	*non-contributing*	0.00000 / 0.0%	*non-contributing*
χ_2	-10.19145	0.00000 / 0.0%	*non-contributing*	0.00000 / 0.0%	*non-contributing*
χ_3	-10.17726	0.00000 / 0.0%	*non-contributing*	0.00000 / 0.0%	*non-contributing*
χ_4	-10.17724	0.00000 / 0.0%	*non-contributing*	0.00000 / 0.0%	*non-contributing*
χ_5	-10.17720	0.00000 / 0.0%	*non-contributing*	0.00000 / 0.0%	*non-contributing*
χ_6	-10.17718	0.00000 / 0.0%	*non-contributing*	0.00000 / 0.0%	*non-contributing*
χ_7	-10.17658	0.00000 / 0.0%	*non-contributing*	0.00000 / 0.0%	*non-contributing*
χ_8	-10.17657	0.00000 / 0.0%	*non-contributing*	0.00000 / 0.0%	*non-contributing*
χ_9	-10.17653	0.00000 / 0.0%	*non-contributing*	0.00000 / 0.0%	*non-contributing*
χ_{10}	-10.17652	0.00000 / 0.0%	*non-contributing*	0.00000 / 0.0%	*non-contributing*
χ_{11}	-10.17586	0.00000 / 0.0%	*non-contributing*	0.00000 / 0.0%	*non-contributing*
χ_{12}	-10.17586	0.00000 / 0.0%	*non-contributing*	0.00000 / 0.0%	*non-contributing*
χ_{13}	-0.87581	0.00031 / 2.2%	*depleting*	0.00017 / 2.3%	*depleting*
χ_{14}	-0.85459	0.00000 / 0.0%	*non-contributing*	0.00000 / 0.0%	*non-contributing*
χ_{15}	-0.78384	0.00028 / 1.9%	*depleting*	0.00014 / 1.9%	*depleting*
χ_{16}	-0.75827	0.00072 / 5.1%	*concentrating*	0.00034 / 4.5%	*depleting*
χ_{17}	-0.74841	0.00000 / 0.0%	*non-contributing*	0.00000 / 0.0%	*non-contributing*
χ_{18}	-0.72791	0.00000 / 0.0%	*non-contributing*	0.00000 / 0.0%	*non-contributing*
χ_{19}	-0.63238	0.00015 / 1.1%	*concentrating*	0.00004 / 0.5%	*concentrating*
χ_{20}	-0.62793	0.00188 / 13.2%	*concentrating*	0.00095 / 12.8%	*depleting*
χ_{21}	-0.59212	0.00000 / 0.0%	*non-contributing*	0.00000 / 0.0%	*non-contributing*
χ_{22}	-0.58592	0.00000 / 0.0%	*non-contributing*	0.00000 / 0.0%	*non-contributing*
χ_{23}	-0.54310	0.00198 / 13.9%	*concentrating*	0.00077 / 10.3%	*concentrating*
χ_{24}	-0.50360	0.00000 / 0.0%	*non-contributing*	0.00000 / 0.0%	*non-contributing*
χ_{25}	-0.48074	0.00237 / 16.6%	*concentrating*	0.00113 / 15.3%	*concentrating*
χ_{26}	-0.47350	0.00019 / 1.3%	*depleting*	0.00019 / 2.6%	*depleting*
χ_{27}	-0.44376	0.00000 / 0.0%	*non-contributing*	0.00000 / 0.0%	*non-contributing*
χ_{28}	-0.43615	0.00000 / 0.0%	*non-contributing*	0.00000 / 0.0%	*non-contributing*
χ_{29}	-0.43567	0.00273 / 19.1%	*concentrating*	0.00111 / 15.0%	*concentrating*
χ_{30}	-0.43051	0.00090 / 6.3%	*concentrating*	0.00050 / 6.8%	*concentrating*

Table S10 continues.

		Planar		Twisted	
MO	Energy (a.u.)	ED contribution (a.u.) / %-fraction	Classification based on 2nd derivative sign (λ_2)	ED contribution (a.u.) / %-fraction	Classification based on 2nd derivative sign (λ_2)
χ_{31}	-0.41671	0.00000 / 0.0%	*non-contributing*	0.00000 / 0.0%	*non-contributing*
χ_{32}	-0.39513	0.00000 / 0.0%	*non-contributing*	0.00000 / 0.0%	*non-contributing*
χ_{33}	-0.36916	0.00000 / 0.0%	*non-contributing*	0.00000 / 0.0%	*non-contributing*
χ_{34}	-0.36616	0.00000 / 0.0%	*non-contributing*	0.00000 / 0.0%	*depleting*
χ_{35}	-0.36285	0.00157 / 11.0%	*concentrating*	0.00083 / 11.2%	*concentrating*
χ_{36}	-0.34790	0.00118 / 8.3%	*concentrating*	0.00066 / 8.6%	*concentrating*
χ_{37}	-0.33466	0.00000 / 0.0%	*non-contributing*	0.00000 / 0.0%	*non-contributing*
χ_{38}	-0.29363	0.00000 / 0.0%	*non-contributing*	0.00000 / 0.0%	*non-contributing*
χ_{39}	-0.26531	0.00000 / 0.0%	*non-contributing*	0.00000 / 0.0%	*non-contributing*
χ_{40}	-0.25903	0.00000 / 0.0%	*non-contributing*	0.00024 / 3.3%	*concentrating*
χ_{41}	-0.23027	0.00000 / 0.0%	*non-contributing*	0.00034 / 4.6%	*depleting*

Table S11. MO-DI data (in e^--pairs) for noncovalent interaction H7···H18 in the planar Bph.

MO	1–24[a]	25	26	27	28	29	30	31	32	33	34	35	36	37	38	39	40	41
1–24	0.005[a]	0.004	0.000	-0.002	0.000	0.005	0.001	-0.002	0.000	-0.002	0.000	0.004	0.001	-0.003	0.000	0.000	0.000	0.000
25	0.004	0.008	0.000	-0.006	0.000	0.009	0.002	-0.006	0.000	-0.004	0.000	0.006	0.002	-0.007	0.000	0.000	0.000	0.000
26	0.000	0.000	0.000	0.000	0.000	0.000	0.000	0.000	0.000	0.000	0.000	0.000	0.000	0.000	0.000	0.000	0.000	0.000
27	-0.002	-0.006	0.000	0.006	0.000	-0.008	-0.002	0.006	0.000	0.003	0.000	-0.005	-0.001	0.007	0.000	0.000	0.000	0.000
28	0.000	0.000	0.000	0.000	0.000	0.000	0.000	0.000	0.000	0.000	0.000	0.000	0.000	0.000	0.000	0.000	0.000	0.000
29	0.005	0.009	0.000	-0.008	0.000	0.012	0.003	-0.008	0.000	-0.005	0.000	0.008	0.002	-0.009	0.000	0.000	0.000	0.000
30	0.001	0.002	0.000	-0.002	0.000	0.003	0.001	-0.002	0.000	-0.001	0.000	0.002	0.001	-0.002	0.000	0.000	0.000	0.000
31	-0.002	-0.006	0.000	0.006	0.000	-0.008	-0.002	0.006	0.000	0.003	0.000	-0.005	-0.001	0.007	0.000	0.000	0.000	0.000
32	0.000	0.000	0.000	0.000	0.000	0.000	0.000	0.000	0.000	0.000	0.000	0.000	0.000	0.000	0.000	0.000	0.000	0.000
33	-0.002	-0.004	0.000	0.003	0.000	-0.005	-0.001	0.003	0.000	0.002	0.000	-0.003	-0.001	0.004	0.000	0.000	0.000	0.000
34	0.000	0.000	0.000	0.000	0.000	0.000	0.000	0.000	0.000	0.000	0.000	0.000	0.000	0.000	0.000	0.000	0.000	0.000
35	0.004	0.006	0.000	-0.005	0.000	0.008	0.002	-0.005	0.000	-0.003	0.000	0.006	0.001	-0.006	0.000	0.000	0.000	0.000
36	0.001	0.002	0.000	-0.001	0.000	0.002	0.001	-0.001	0.000	-0.001	0.000	0.001	0.001	-0.001	0.000	0.000	0.000	0.000
37	-0.003	-0.007	0.000	0.007	0.000	-0.009	-0.002	0.007	0.000	0.004	0.000	-0.006	-0.001	0.008	0.000	0.000	0.000	0.000
38	0.000	0.000	0.000	0.000	0.000	0.000	0.000	0.000	0.000	0.000	0.000	0.000	0.000	0.000	0.000	0.000	0.000	0.000
39	0.000	0.000	0.000	0.000	0.000	0.000	0.000	0.000	0.000	0.000	0.000	0.000	0.000	0.000	0.000	0.000	0.000	0.000
40	0.000	0.000	0.000	0.000	0.000	0.000	0.000	0.000	0.000	0.000	0.000	0.000	0.000	0.000	0.000	0.000	0.000	0.000
41	0.000	0.000	0.000	0.000	0.000	0.000	0.000	0.000	0.000	0.000	0.000	0.000	0.000	0.000	0.000	0.000	0.000	0.000
Diagonal	0.015[a]	0.008	0.000	0.006	0.000	0.012	0.001	0.006	0.000	0.002	0.000	0.006	0.001	0.008	0.000	0.000	0.000	0.000
Off-diagonal	-0.004[a]	0.001	0.000	-0.009	0.000	-0.002	0.002	-0.009	0.000	-0.004	0.000	0.001	0.002	-0.011	0.000	0.000	0.000	0.000
Total	0.011	0.008	0.000	-0.003	0.000	0.010	0.003	-0.003	0.000	-0.002	0.000	0.007	0.003	-0.003	0.000	0.000	0.000	0.000

[a] MOs 1–24 were combined for the sake of brevity. The contributions made by diagonal elements of these MOs equal 0.015, whereas off-diagonal terms of only these MOs equal –0.01 to give a net contribution of 0.05. Interference with the remaining MOs (MOs 25–41) gives a positive, off-diagonal contribution of +0.006, so that the total contribution of MOs 1–24 equals 0.011.

Table S12. MO-DI data (in e^--pairs) for noncovalent interaction H7···H18 in the twisted Bph.

MO	1–24[a]	25	26	27	28	29	30	31	32	33	34	35	36	37	38	39	40	41
1–24	0.001[a]	0.004	0.000	-0.002	0.000	0.005	0.001	-0.002	0.000	-0.002	0.000	0.004	0.001	-0.003	0.000	0.000	0.000	0.000
25	0.000	0.008	0.000	-0.007	0.000	0.008	0.003	-0.007	-0.001	-0.003	0.000	0.007	0.002	-0.007	0.000	0.000	0.000	0.000
26	0.000	0.000	0.000	0.000	0.000	0.000	0.000	0.000	0.000	0.000	0.000	0.000	0.000	0.000	0.000	0.000	0.000	0.000
27	0.001	-0.007	0.000	0.006	0.000	-0.007	-0.002	0.006	0.001	0.003	0.000	-0.006	-0.002	0.007	0.000	0.000	0.000	0.000
28	0.000	0.000	0.000	0.000	0.000	0.000	0.000	0.000	0.000	0.000	0.000	0.000	0.000	0.000	0.000	0.000	0.000	0.000
29	0.000	0.008	0.000	-0.007	0.000	0.009	0.003	-0.007	-0.001	-0.003	0.000	0.007	0.002	-0.008	0.000	0.000	0.000	0.000
30	0.000	0.003	0.000	-0.002	0.000	0.003	0.001	-0.002	0.000	-0.001	0.000	0.002	0.001	-0.002	0.000	0.000	0.000	0.000
31	0.001	-0.007	0.000	0.006	0.000	-0.007	-0.002	0.006	0.001	0.003	0.000	-0.006	-0.002	0.007	0.000	0.000	0.000	0.000
32	0.000	-0.001	0.000	0.001	0.000	-0.001	0.000	0.001	0.000	0.000	0.000	-0.001	0.000	0.001	0.000	0.000	0.000	0.000
33	0.000	-0.003	0.000	0.003	0.000	-0.003	-0.001	0.003	0.000	0.001	0.000	-0.003	-0.001	0.003	0.000	0.000	0.000	0.000
34	0.000	0.000	0.000	0.000	0.000	0.000	0.000	0.000	0.000	0.000	0.000	0.000	0.000	-0.001	0.000	0.000	0.000	0.000
35	0.000	0.007	0.000	-0.006	0.000	0.007	0.002	-0.006	-0.001	-0.003	0.000	0.006	0.002	-0.006	0.000	0.000	0.000	0.000
36	0.000	0.002	0.000	-0.002	0.000	0.002	0.001	-0.002	0.000	-0.001	0.000	0.002	0.001	-0.002	0.000	0.000	0.000	0.000
37	0.001	-0.007	0.000	0.007	0.000	-0.008	-0.002	0.007	0.001	0.003	-0.001	-0.006	-0.002	0.007	0.000	0.000	0.000	0.000
38	0.000	0.000	0.000	0.000	0.000	0.000	0.000	0.000	0.000	0.000	0.000	0.000	0.000	0.000	0.000	0.000	0.000	0.000
39	0.000	0.000	0.000	0.000	0.000	0.000	0.000	0.000	0.000	0.000	0.000	0.000	0.000	0.000	0.000	0.000	0.000	0.000
40	0.000	0.000	0.000	0.000	0.000	0.000	0.000	0.000	0.000	0.000	0.000	0.000	0.000	0.000	0.000	0.000	0.000	0.000
41	0.000	0.000	0.000	0.000	0.000	0.000	0.000	0.000	0.000	0.000	0.000	0.000	0.000	0.000	0.000	0.000	0.000	0.000
Diagonal	0.014[a]	0.008	0.000	0.006	0.000	0.009	0.001	0.006	0.000	0.001	0.000	0.006	0.001	0.007	0.000	0.000	0.000	0.000
Off-diagonal	-0.011	-0.005	0.000	-0.007	0.000	-0.005	0.000	-0.007	0.000	-0.002	0.000	-0.003	0.001	-0.008	0.000	0.000	0.000	0.000
Total	0.003	0.003	0.000	-0.001	0.000	0.003	0.001	-0.001	0.000	-0.001	0.000	0.003	0.001	-0.001	0.000	0.000	0.000	0.000

[a] MOs 1–24 were combined for the sake of brevity. The contributions made by diagonal elements of these MOs equal 0.014, whereas off-diagonal terms of only these MOs equal –0.013 to give a net contribution of 0.001. Interference with the remaining MOs (MOs 25–41) gives a positive, off-diagonal contribution of +0.002, so that the total contribution of MOs 1–24 equals 0.003.

Table S13. Summary of MO-ED & MO-DI data for H7···H18 in planar and twisted Bph

	Planar		Twisted	
Classification based on λ_2	**Number of MOs**	**Contribution to ρ(CP)[a]**	**Number of MOs**	**Contribution to ρ(MDP)[a]**
Concentrating	9	0.013	8	0.005
Depleting	3	0.001	7	0.002
Non-contributing	29	0.000	26	0.000
Delocalization		**Contribution to DI[b]**		**Contribution to DI[b]**
Overlapping		0.064		0.060
Interference		–0.033		–0.049
Net DI		0.031		0.011

[a] in a.u.; [b] in e^--pairs.

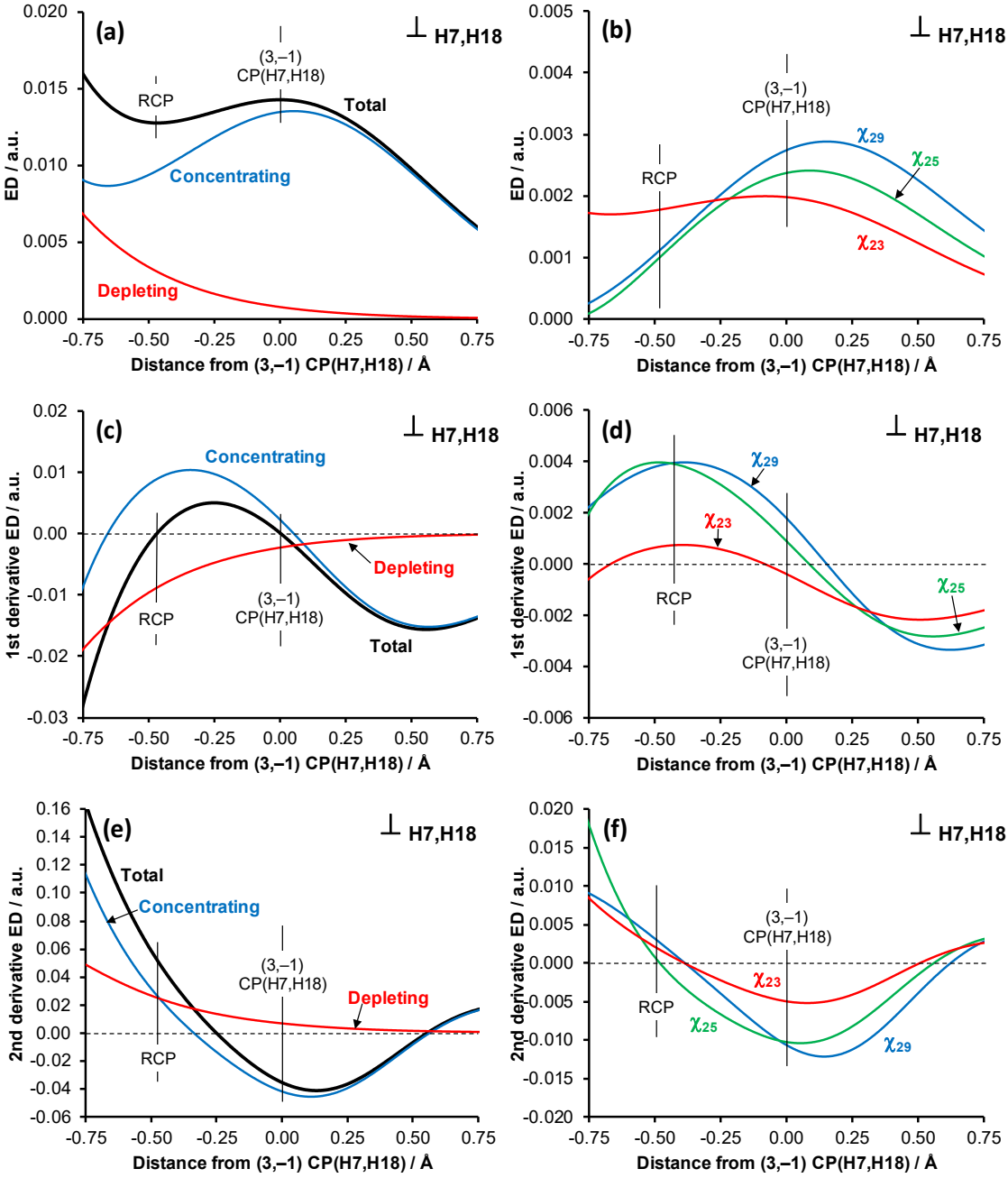

Figure S5. Decomposition of the total-ED (**a**), first derivative (**c**) and directional partial derivatives (**e**) along the λ_2–eigenvector in the H7,H18 inter-nuclear region in planar biphenyl, as well as the subsequent decomposition of the concentrating density into the largest MO contributions (**b,d,f)**

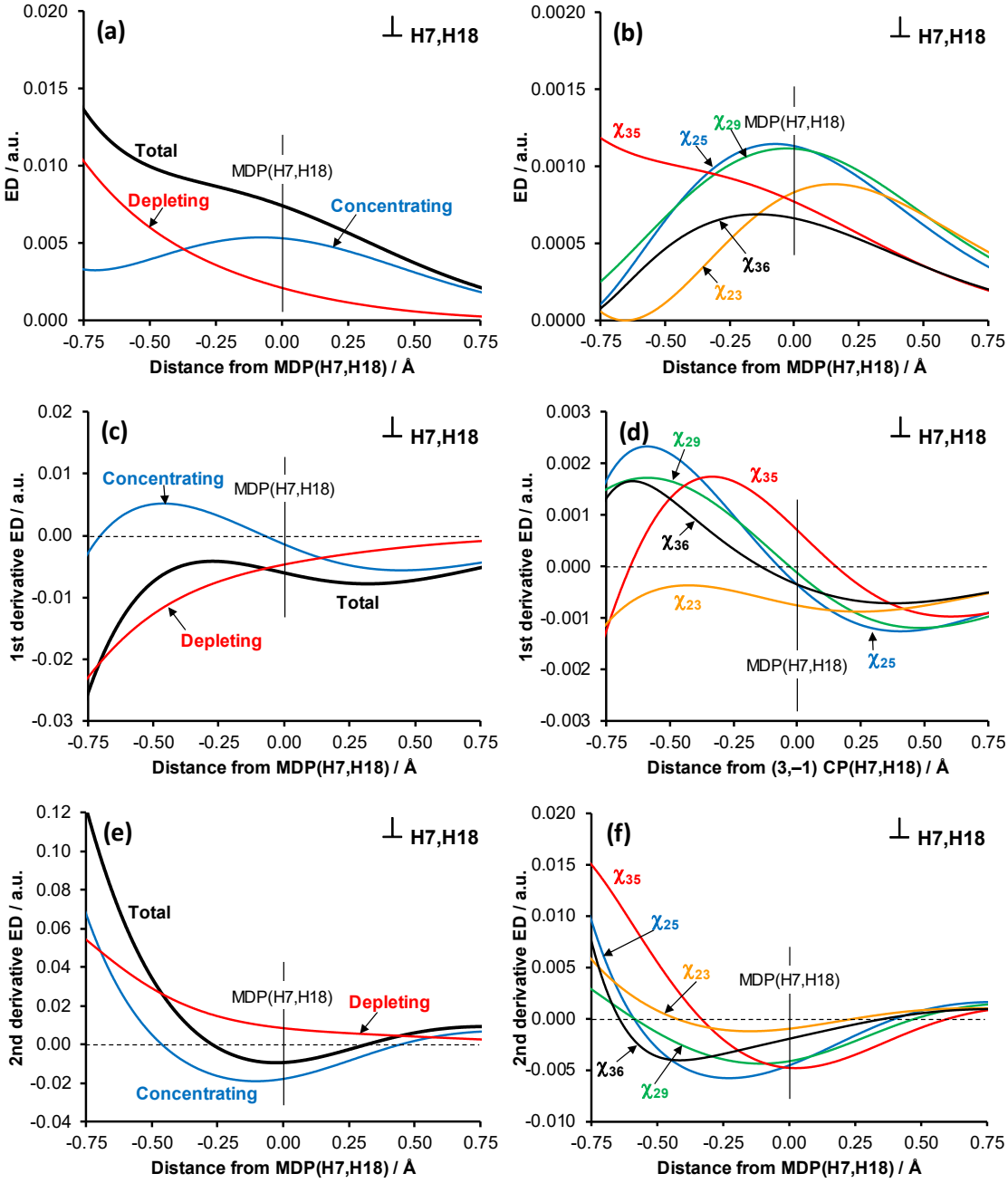

Figure S6. Decomposition of the total-ED (**a**), first derivative (**c**) and directional partial derivatives (**e**) along the λ_2–eigenvector in the H7,H18 inter-nuclear region in twisted biphenyl, as well as the subsequent decomposition of the concentrating density into the largest MO contributions (**b,d,f)**

End of Part 5

Part 6 – Data pertaining to H ··H density bridges in Li_4H_4

Table S14. MO-ED data at (3,–1) CP(H2,H4), CP(H2,H5) and CP(H4,H5) in Li_4H_4.

		H2,H4		**H2,H5**		**H4,H5**	
MO	Energy (a.u.)	ED contribution (a.u.) / %-fraction	Classification based on 2nd derivative sign (λ_2)	ED contribution (a.u.) / %-fraction	Classification based on 2nd derivative sign (λ_2)	ED contribution (a.u.) / %-fraction	Classification based on 2nd derivative sign (λ_2)
χ_1	-10.19173	0.00013 / 0.8%	*Depleting*	0.00013 / 0.8%	*Depleting*	0.00013 / 0.8%	*Depleting*
χ_2	-10.19145	0.00005 / 0.3%	*Depleting*	0.00005 / 0.3%	*Depleting*	0.00003 / 0.2%	*Depleting*
χ_3	-10.17726	0.00002 / 0.1%	*Depleting*	0.00001 / 0.1%	*Depleting*	0.00010 / 0.7%	*Depleting*
χ_4	-10.17724	0.00006 / 0.4%	*Depleting*	0.00007 / 0.5%	*Depleting*	0.00000 / 0.0%	*Non-Contributing*
χ_5	-10.17720	0.00829 / 54.2%	*Concentrating*	0.00829 / 54.2%	*Concentrating*	0.00829 / 54.2%	*Concentrating*
χ_6	-10.17718	0.00000 / 0.0%	*Non-Contributing*	0.00158 / 10.4%	*Concentrating*	0.00516 / 33.8%	*Concentrating*
χ_7	-10.17658	0.00369 / 24.2%	*Concentrating*	0.00226 / 14.8%	*Concentrating*	0.00079 / 5.2%	*Concentrating*
χ_8	-10.17657	0.00305 / 20.0%	*Concentrating*	0.00290 / 19.0%	*Concentrating*	0.00079 / 5.2%	*Concentrating*

Table S15. MO-DI data for the H2,H5 atom-pair in Li_4H_4.

MO	MO1	MO2	MO3	MO4	MO5	MO6	MO7	MO8
MO1	0.000	0.000	0.000	0.000	0.001	0.000	0.000	0.000
MO2	0.000	0.000	0.000	0.000	0.000	0.000	0.000	0.000
MO3	0.000	0.000	0.000	0.000	0.000	0.000	0.000	0.000
MO4	0.000	0.000	0.000	0.000	0.000	0.000	0.000	0.000
MO5	0.001	0.000	0.000	0.000	0.207	-0.029	-0.057	-0.103
MO6	0.000	0.000	0.000	0.000	-0.029	0.009	0.009	0.016
MO7	0.000	0.000	0.000	0.000	-0.057	0.009	0.051	0.032
MO8	0.000	0.000	0.000	0.000	-0.103	0.016	0.032	0.092
Diagonal	0.000	0.000	0.000	0.000	0.207	0.009	0.051	0.092
Off-diagonal	0.000	0.000	0.000	0.000	-0.189	-0.004	-0.016	-0.055
Total	0.000	0.000	0.000	0.000	0.018	0.005	0.035	0.037

Table S16. Summary of MO-ED and MO-DI data for three H···H density bridges in Li_4H_4.

	H2,H4		H2,H5		H4,H5	
Classification based on λ_2	**Number of MOs**	**Contribution to ρ(CP)[a]**	**Number of MOs**	**Contribution to ρ(CP)[a]**	**Number of MOs**	**Contribution to ρ(CP)[a]**
Concentrating	3	0.015	4	0.015	4	0.015
Depleting	4	0.000	4	0.000	3	0.000
Non-contributing	1	0.000	0	0.000	1	0.000
Delocalization		**Contribution to DI[b]**		**Contribution to DI[b]**		**Contribution to DI[b]**
Overlapping		0.36		0.36		0.36
Interference		–0.26		–0.26		–0.26
Net DI		0.09		0.09		0.09

[a] in a.u.; [b] in e^--pairs.

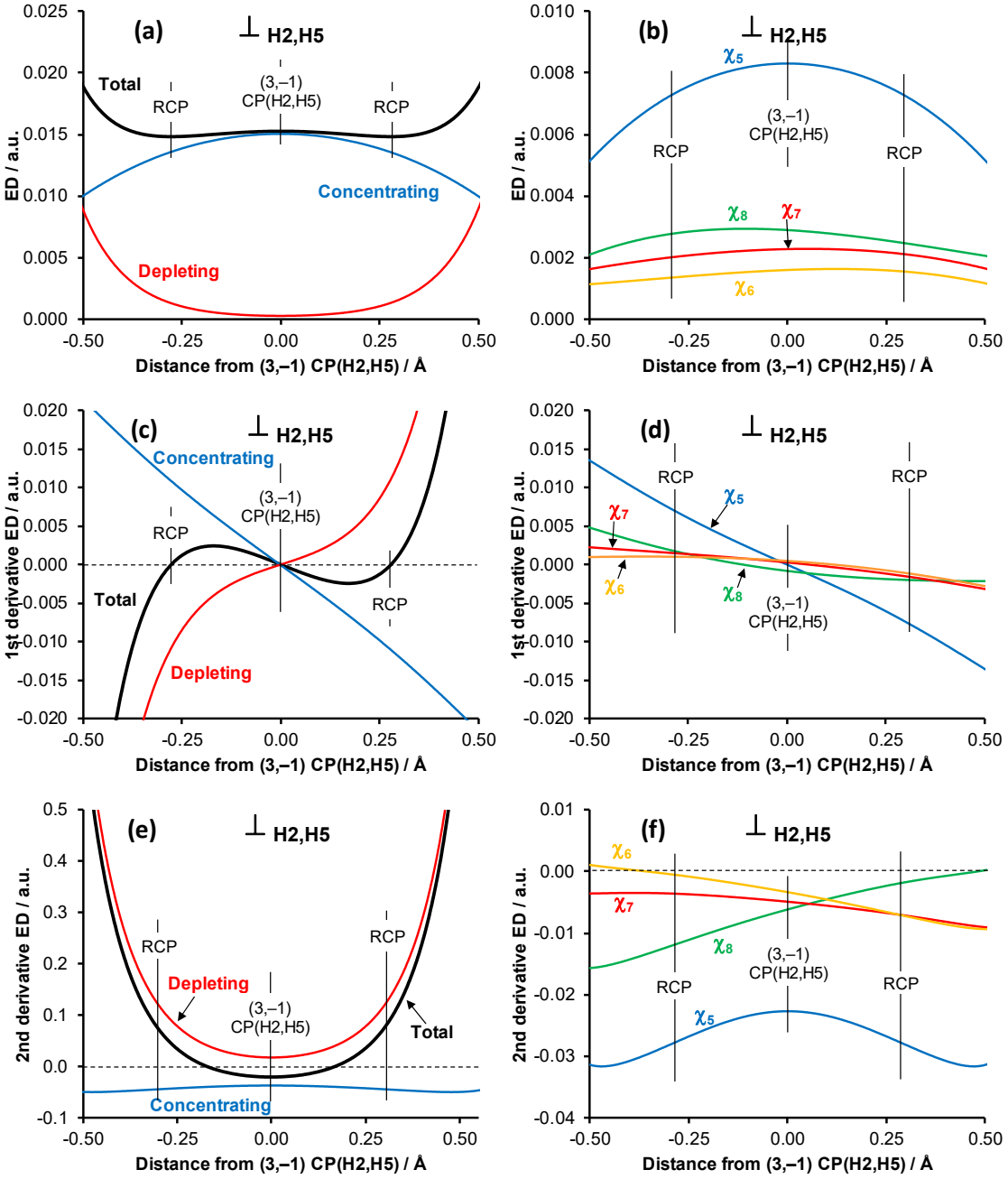

Figure S7. Decomposition of the total-ED (**a**), first derivative (**c**) and directional partial derivatives (**e**) along the λ_2–eigenvector in the H2,H5 inter-nuclear region in Li_4H_4, as well as the subsequent decomposition of the concentrating density into the largest MO contributions (**b,d,f**).

End of Part 6